# Artificial Photosynthesis: An Investigation of Silicon Nanowires in Nickel Catalyzed Carboxylation

Author: Carolynn Kay Stephani

Boston College

The Graduate School of Arts and Sciences

Department of Chemistry

# ARTIFICIAL PHOTOSYNTHESIS: AN INVESTIGATION OF SILICON NANOWIRES IN NICKEL CATALYZED CARBOXYLATION

a thesis

by

CAROLYNN STEPHANI

submitted in partial fulfillment of the requirements

for the degree of

Master of Science

May 2014

# Artificial Photosynthesis: An Investigation of Silicon Nanowires in Nickel Catalyzed Carboxylation

Carolynn Stephani

Thesis Advisors: Dr. Kian L. Tan and Dr. Dunwei Wang

**Abstract.** Silicon nanowires are utilized to harvest the energy from visible light. The introduction of a nickel pre-catalyst, **1**, allows for this energy to be stored in chemical bonds, which are subsequently used in the carboxylation of 4-octyne.

**Acknowledgements**

I would like to express my gratitude to Dr. Kian L. Tan and Dr. Dunwei Wang for their mentorship in my time at Boston College. Their thoughtfulness, patience, and leadership have been invaluable to me, and have shown me how to face great challenges both in science and in life. I would like to thank Frank Tsung for taking the time to read my thesis, as well as for always being an open source of communication. I would also like to thank my high school physics teacher, Mr. Morgan, for his emphatic encouragement to pursue the sciences. My thanks go to Rui Liu, who was a great partner in this project. My thanks also go to Guangbi Yuan for his guidance in the project. Special thanks go to Tom Blaisdell and Candice Joe for being ever-present sources of guidance and cheerfulness in the lab, and for their warm friendship. To the other members of the Tan and Wang group, I thank you for discussions and for making Merkert Chemistry Center a welcoming place to work. Finally, thanks to my family and friends for all their encouragement and support during my time here.

## Table of Contents

## List of Abbreviations

| | |
|---|---|
| 3PG | 3-Phosphoglycerate |
| Ac | Acetyl |
| ACS | American Chemical Society |
| Ar | Aryl |
| ATP | Adenosine triphosphate |
| bpy | 2,2'-Bipyridine |
| C | Capacitance |
| c- | Cyclic |
| CO | Carbon monoxide |
| $CO_2$ | Carbon dioxide |
| COD | Cyclooctadiene |
| Cy | Cyclohexyl |
| d | doublet |
| DABCO | 1,4-Diazabicyclo[2.2.2]octane |
| dbu | 1,8-Diazabicycloundec-7-ene |
| DI | Deionized |
| DMF | Dimethylformamide |
| dt | doublet of triplets |
| ε | Dielectric constant |
| $\varepsilon_0$ | Permittivity of a vacuum |
| EIS | Electrochemical impedance spectroscopy |
| Et | Ethyl |

| | |
|---|---|
| GAP | Glyceraldehyde 3-phosphate |
| GC | Gas chromatography |
| h | hours |
| Hex | Hexane |
| HRMS | High resolution mass spectrometry |
| k | Botzmann constant |
| LAH | Lithium aluminum hydride |
| m | multiplet |
| MeOH | Methanol |
| *n*- | Normal |
| $N_A$ | Hole density |
| NADPH | Adenine dinucleotide phosphate |
| NMR | Nuclear magnetic resonance |
| PEC | Photoelectrochemical |
| Ph | Phenyl |
| Py | Pyridine |
| q | Electron charge |
| RuBP | 1,5-Bisphosphate |
| SCE | Saturated calomel electrode |
| SiNW | Silicon nanowire |
| T | Temperature |
| *t*- | tert |
| THF | Tetrahydrofuran |

| | |
|---|---|
| TMEDA | Tetramethylethylenediamine |
| TMS | Trimethylsilyl ether |
| V | Applied potential |

## I. $CO_2$ Reduction

The increased release of carbon dioxide ($CO_2$) in the atmosphere has attracted attention by the scientific community as well as the general public. The growing necessity to reduce the amount of $CO_2$ has catalyzed interest into converting $CO_2$ into a useful state by activation and reduction in order to convert it to valuable products. Both thermodynamic and kinetic challenges plague the direct reduction of $CO_2$. This is manifested in the high overpotentials required to complete the multielectron transfer from $CO_2$ to other carbon-based products. Additionally, a variety of carbon products can be obtained from this direct reduction (Scheme 1),[1] and therefore product selectivity can be difficult to obtain.

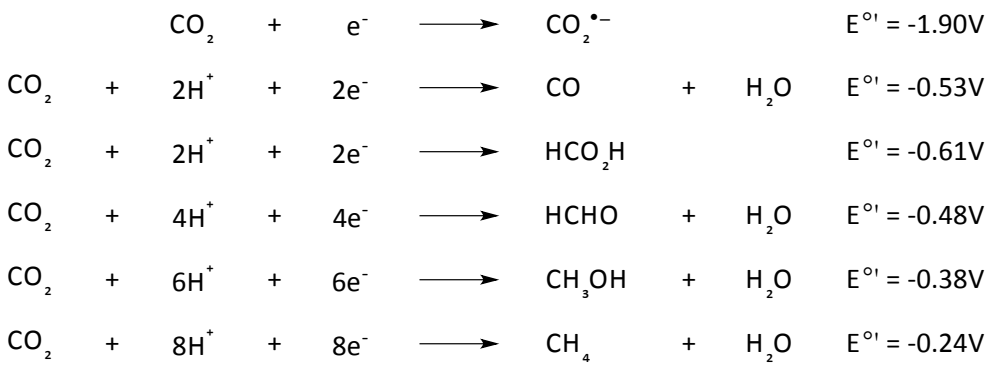


**Scheme 1** Possible products of the direct reduction of $CO_2$ and the overpotentials required to obtain them.

Much work has been done to overcome these challenges, specifically for the formation of fuels.[2,3] An alternative approach involves the direct incorporation of $CO_2$ into organic molecules, to afford synthetically valuable compounds. This solution lies in the concept of indirectly reducing $CO_2$. One prominent example of this is in the process of photosynthesis.

---

[1] Schneider, J.; Jia, H.; Muckerman, J. T.; Fujita, E. *Chem. Soc. Rev.* **2012**, *41*, 2036.
[2] Alstrum-Acevedo, J. H.; Brennaman, M. K.; Meyer, T. J. *Inorg. Chem.* **2005**, *44*, 6802.
[3] Benson, E. E.; Kubiak, C. P.; Sathrum, A. J.; Smieja, J. M. *Chem. Soc. Rev.* **2009**, *38*, 89.

## II. Photosynthesis

In natural photosynthesis, solar energy is converted to chemical energy in a two-part process, the light reactions and the dark reactions (Scheme 2).[4]

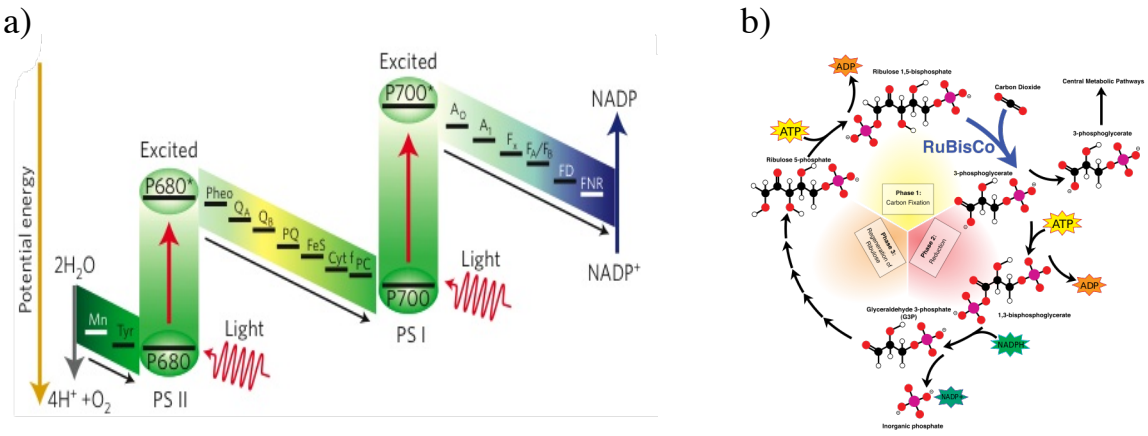


**Scheme 2** Adapted from reference 4. Natural Photosynthesis process includes a) the light reaction, and b) the dark reaction (Calvin cycle).

In the light reactions (Scheme 2a), a photon of light is absorbed by the chlorophyll in plants, causing an electron to be excited in the reaction center of the photosynthesis machinery. This excited electron undergoes a series of redox reactions, generating a potential across the cell membrane, the energy of which is used in the formation of the small molecule adenosine triphosphate (ATP). The final redox reaction forms a second small molecule, nicotinamide adenine dinucleotide phosphate (NADPH). In this way, the energy from the light is stored in the chemical bonds of small molecules. These small molecules then go on to participate in the dark reactions (Scheme 2b), which allows for the energy stored in the chemical bonds to be transferred to the formation of sugars. In the dark reaction,[5] a small molecule,

[4] Barber, J.; Tran, P. D. *J. R. Soc. Interface* **2013**, *10*, 81.
[5] Sillero, A.; Selivanov, V. A.; Cascante, M. *Biochem. Mol. Biol. Educ.* **2006**, *34*, 275.

ribulose 1,5-bisphosphate (RuBP), incorporates a molecule of $CO_2$. The subsequent molecule immediately breaks into two, forming two molecules of 3-phosphoglycerate (3PG). The 3PG is then phosphorylated through the use of ATP, and reduced by NADPH to form glyceraldehyde 3-phosphate (GAP), a precursor to glucose and other sugars. Finally, additional ATP is used to regenerate the original $CO_2$ accepting molecule, RuBP.

In this two-part process, photosynthesis acknowledges that carbon-carbon bond formation is not compatible with a light-harvesting mechanism. Instead, it employs two distinct, well-honed systems to separate harvesting energy and synthesizing organic products, allowing for precise control over each reaction. Encompassed in this system is the indirect reduction of $CO_2$. By utilizing the abundant energy found in light, photosynthesis is able to overcome the thermodynamic challenges of $CO_2$ reduction. Additionally, it is able to overcome the kinetic challenges by first incorporating $CO_2$ into a molecule prior to reduction, allowing for product selectivity. Applying such a light harvesting technique in a laboratory setting could be advantageous, in that visible light is very abundant, and if this could be utilized, one would have access to large amounts of readily available energy. However, it can be difficult to control the rate at which this light is absorbed and utilized in a reaction, thus making the kinetics of a reaction difficult to control. It would therefore be very powerful if, similar to photosynthesis, the light harvesting mechanism could be adequately separated from the synthesis mechanism, allowing for control of product selectivity.

**III. Photoelectrochemistry**

It was the goal of the joint project between the Tan Group and Wang Group to apply the concept of storing energy from light in chemical bonds and converting it to organic reactions for the synthesis of useful organic molecules. Additionally, to further the parallel of photosynthesis, it was desired to incorporate the indirect reduction of $CO_2$. In doing so, a light-harvesting motif was necessary in order to harvest solar energy and separate charges. When looking at charge separation, it is natural to turn to the use of semiconductors.[6] Many semiconductors are able to absorb broadly in the visible light range, in accordance with the size of their band gap. When this occurs, electrons are pumped from the valence band to the conduction band. Additionally, when a semiconductor comes into contact with an electrolytic solution, there is a flow of charge between the substrate and the solution. This flow of charge generates a depletion layer in the semiconductor near the semiconductor/solution interface, and results in bending of the band gap. These factors present a mechanism that allows for the separation of photoexcited charges. Due to this ability to separate charges, semiconductors have been used as photoelectrodes in artificial photosynthesis in the form of photoelectrochemical (PEC) cells.[7-10] Despite this work, however, finding a system that offers all of the desired properties of light absorption, charge separation, and catalytic activity simultaneously remains a challenge. Several techniques have been investigated to overcome these challenges, including control of material synthesis, manipulation of

[6] Lewis, N. S. *Inorg. Chem.* **2005**, *44*, 6900.
[7] Bar-Even, A.; Noor E.; Lewis, N. E.; Milo, R. *Proc. Natl. Acad. Sci. U.S.A.* **2010**, *107*, 8889.
[8] Cole, E. B.; Lakkaraju, P. S.; Rampulla, D. M.; Morris, A. J.; Abelev, E.; Bocarsly, A. B. *J. Am. Chem. Soc.* **2010**, *132*, 11539.
[9] Kuhl, K. P.; Cave, E. R.; Abram, D. N.; Jaramillo, T. F. *Energy Environ. Sci.* **2012**, *5*, 7050.
[10] House, R.; Alibabaei, L.; Bonino, C.; Hoertz, P.; Trainham, J.; Meyer, T. *PV Magazine*, **2013**, *3*, 87.

material morphology, and utilization of catalysts through either semiconductor/catalyst heterojunction systems or the introduction of homogeneous reaction catalysts.

The Wang and Tan groups first took the approach of utilizing semiconductors in the application of storing photonic energy for its use in organic reactions by demonstrating carboxylation reactions using light as a direct energy source and $CO_2$ as a carbon source.[11] In this work, SiNWs were used for the reduction of aromatic ketones. The precursors for the anti-inflammatory drugs naproxen and ibuprofen, 2-acetyl-6-methoxynaphthalene and 4-isobutylacetophenone, respectively, were reduced in both high yield and selectivity (Figure 1).

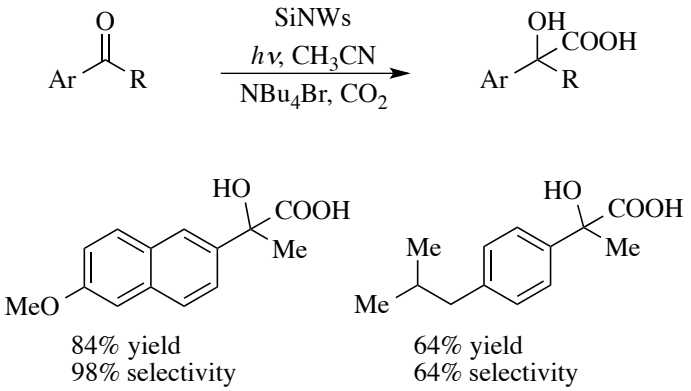


**Figure 1** Selectivity and isolated yields for 2-acetyl-6-methoxynaphthalene and 4-isobutylacetophenone.

This work highlights the ability to power a chemical reaction utilizing light, as well as the ability to use $CO_2$ as a primary carbon source in the formation of synthetically relevant molecules. Additionally, it demonstrates the applicability of SiNWs for high-efficiency PEC operations. This is seen in the less-negative turn-on potential on SiNWs relative to both planar Si and Pt, a commonly used electrode (Figure 2).

[11] Liu, R.; Yuan, G.; Joe, C. L.; Lightburn, T. E.; Tan, K. L.; Wang, D. *Angew. Chem. Int. Ed.* **2012**, *51*, 6709.

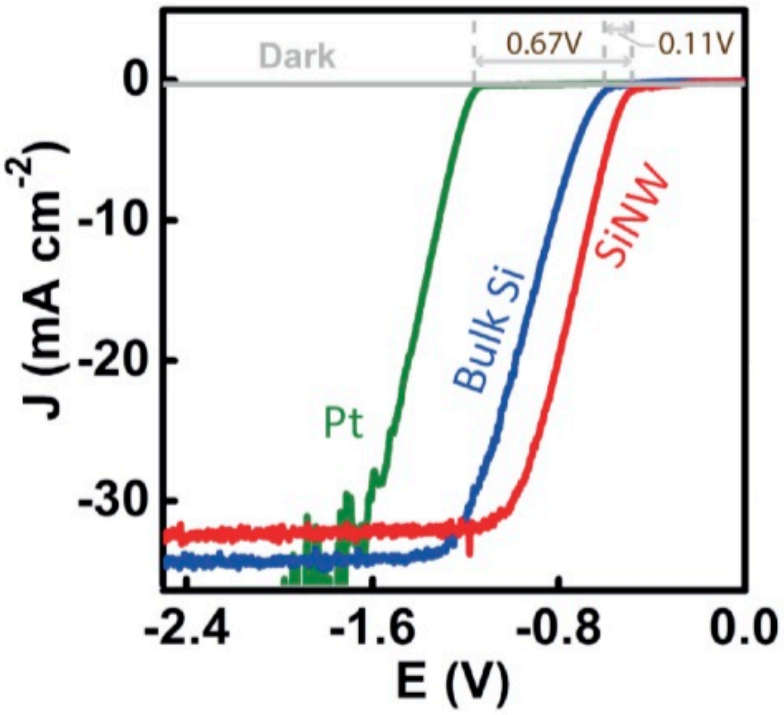


**Figure 2** Adapted from reference 11. Photochemical characteristics of benzilic acid formation by p-type SiNWs. Compared with Pt and planar Si substrate, p-type SiNWs exhibit less negative turn-on voltages. Data was obtained under 100 mW $cm^{-2}$ AM 1.5G illumination.

This improved performance on SiNWs is believed to derive from the improved charge transfer kinetics on the SiNWs due to their multifaceted nature. Ultimately, it was determined that this system was comparable to or better than other reported electrochemical carboxylation techniques.

**IV. Nickel Reactions**

While the aromatic ketone reduction was a good demonstration of harvesting the energy from light to power synthetic reactions, it did not encompass the concept of separating the energy harvesting mechanism from the synthesis process. Rather than storing the photonic energy in the form of chemical bonds which could continue on to complete a dark reaction, the photonic energy was used directly to reduce a molecule in one light reaction. It was thus envisioned that, through

incorporation of a catalyst, the photonic energy could be stored in the chemical bonds of the catalyst, which would then go on to complete an organic reaction. Several transition metals have been shown to be capable of reducing $CO_2$,[12-13] and one metal that has been shown to be particularly prodigious in the formation of carbon-carbon bonds between $CO_2$ and organic groups is nickel. Through the use of nickel catalysts, a wide variety of products can be accessed.

Throughout the 1980's and into the early '90s, the Hoberg Group published a series of papers demonstrating alkyne and alkene carboxylation through the use of stoichiometric Ni(0) complexes and $CO_2$.[14-24] In 1984 they isolated the first nickelacycle[25] through introduction of alkynes and $CO_2$ into electron rich Ni(0). It was demonstrated that, after formation of the nickelacycle, several products could be accessed by controlling the subsequent reaction conditions (Scheme 3).

[12] Walther, D. *Coord. Chem. Rev.* **1987**, *79*, 135.
[13] Braunstein, P.; Matt, D.; Nobel, D. *Chem. Rev.* **1988**, *88*, 747.
[14] Burkhart, G.; Hoberg, H. *Angew. Chem.* **1982**, *94*, 75.
[15] Hoberg, H.; Schaefer, D. *J. of Organomet. Chem.* **1982**, *236*, C28.
[16] Hoberg, H.; Schaefer, D. *J. of Organomet. Chem.* **1982**, *238*, 383.
[17] Hoberg, H.; Schaefer, D. *J. of Organomet. Chem.* **1983**, *255*, C15.
[18] Hoberg, H.; Schaefer, D. *J. of Organomet. Chem.* **1983**, *251*, C51.
[19] Hoberg, H.; Peres, Y., Milchereit, A. *J. of Organomet. Chem.* **1986**, *307*, C38.
[20] Hoberg, H.; Peres, Y.; Milchereit, A. *J. of Organomet. Chem.* **1986**, *307*, C41.
[21] Hoberg, H.; Groβ, S.; Milchereit, A. *Angew. Chem.* **1987**, *99*, 567.
[22] Hoberg, H.; Peres, Y.; Krüger, C.; Tsay, Y.-H. *Angew. Chem.* **1987**, *99*, 799.
[23] Hoberg, H.; Peres, Y.; Milchereit, A.; Gross, S. *J. of Organomet. Chem.* **1988**, *347*, C17.
[24] Hoberg H.; Ballesteros, A. *J. of Organomet. Chem.* **1991**, *411*, C11.
[25] Hoberg, H.; Schaefer, D.; Burkart, G.; Krüger, C.; Romão, M. J. *J. of Organomet. Chem.* **1984**, *266*, 203.

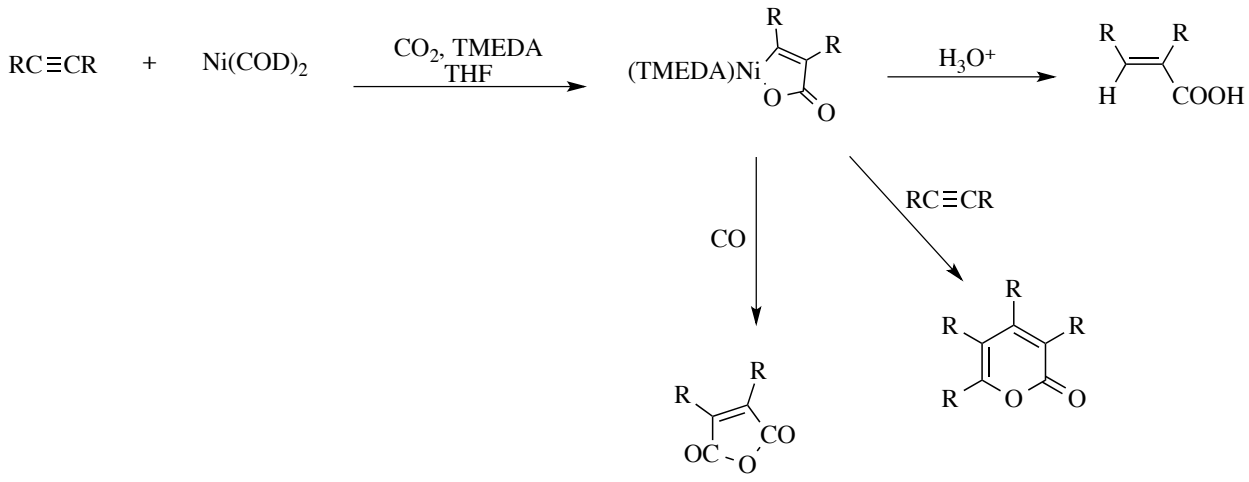


**Scheme 3** Complexation of Ni(0) with alkyne and $CO_2$ leads to an isolatable Ni(II) metallacycle. Control of the subsequent reaction allows for the formation of a substituted carboxylic acid, a lactone, or an anhydride.

Direct hydrolysis of the metallacycle yielded a substituted carboxylic acid, while introduction of a second molecule of alkyne led to the oligomerized lactone product. Additionally, insertion of CO resulted in the formation of an anhydride. It was later shown that such metallacycles could be isolated for both terminal and internal alkynes, as well as alkenes.[20] The nickelacycle formed from alkenes could be converted into substituted carboxylic acids through the addition of acid (Figure 3).

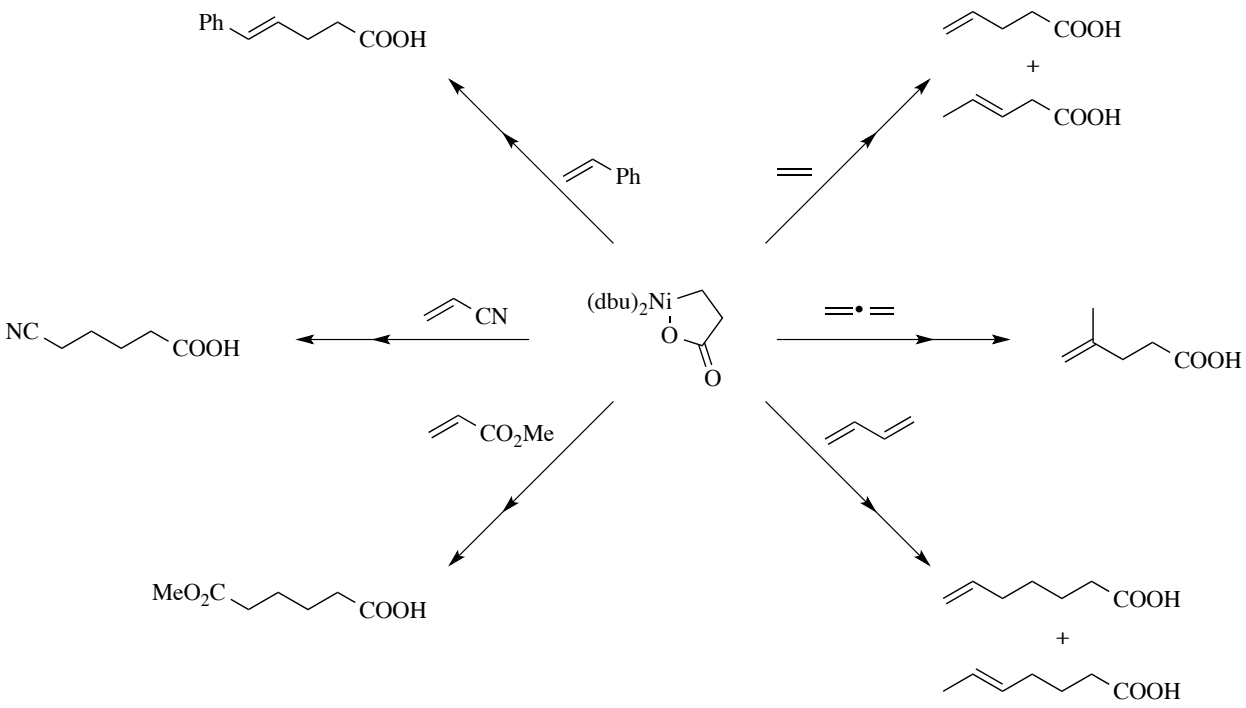


**Figure 3** Complexation of Ni(0) with ethylene and $CO_2$ leads to an isolatable Ni(II) metallacycle. Further reaction with alkenes allows access to a variety of substituted carboxylic acids.

The Mori group later demonstrated a similar reaction to be catalytic in nickel (Scheme 4).[26]

[26] Shimizu, K.; Takimoto, M.; Sato, Y.; Mori, M. *Org. Lett.* **2005**, *7*, 195.

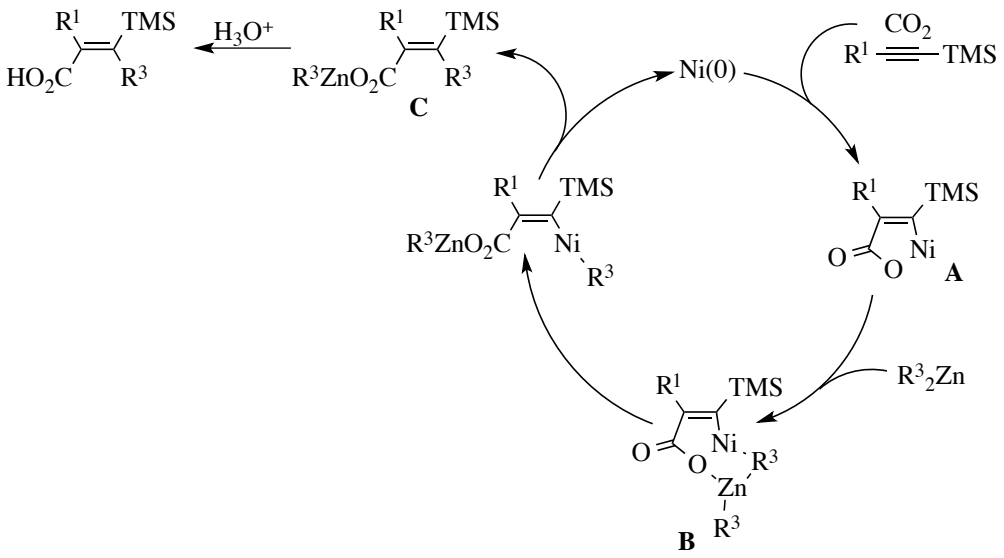


**Scheme 4** Complexation of Ni(0) with internal alkynes and $CO_2$ leads to a Ni(II) metallacycle. Transmetallation with a dialkyl zinc reagent and subsequent product liberation yields a substituted carboxylic acid and regenerateds the Ni(0) species.

In this reaction, internal alkynes and $CO_2$ were inserted into a catalytic Ni(0) source, forming a nickelacycle intermediate (**A**). This intermediate was then transmetallated with a dialkyl zinc reagent to give an alkylnickel complex (**B**), which undergoes reductive elimination to regenerate the Ni(0) catalyst and yield a zinc carboxylate (**C**). The formation of the thermodynamically stable metallacycle intermediate (**A**) was able to control the regioselectivity of the $CO_2$ insertion. Despite being catalytic in Ni, the necessity of harsh dialkyl zinc reagents to facilitate cleavage of the carboxylic acid product from the metal center make the reaction less

than ideal.

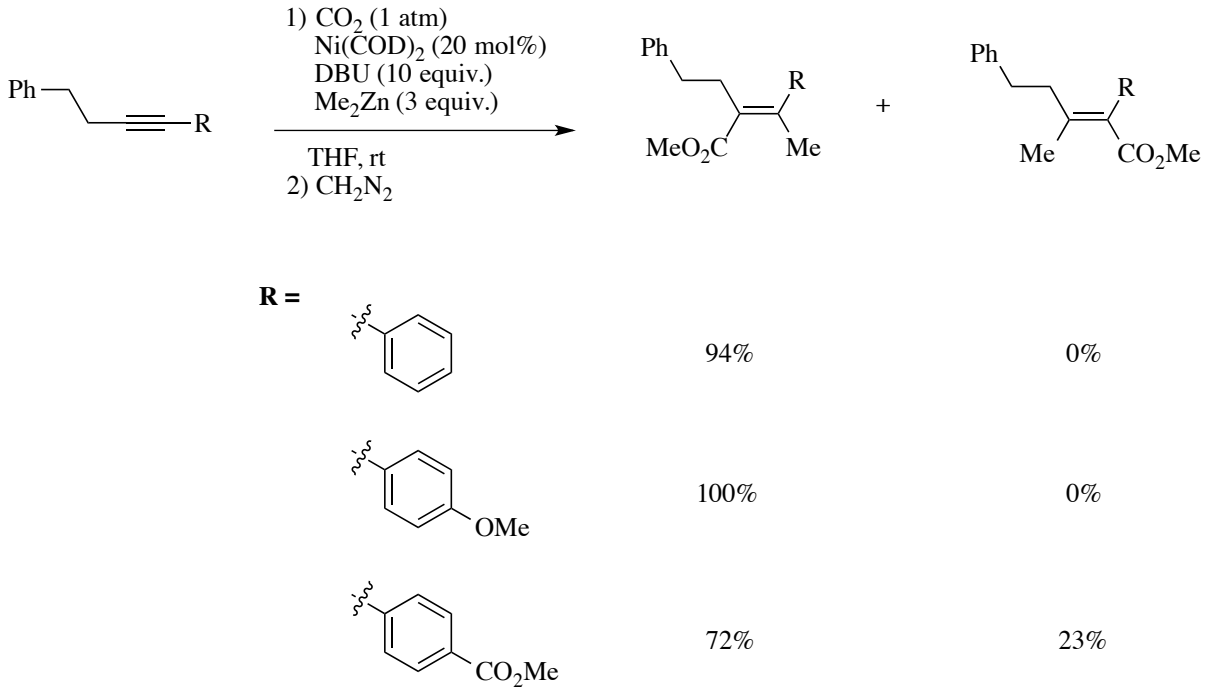


**Figure 4** Isolated yields of the selective carboxylation of internal alkynes.

In 1991, Duñach and Périchon showed a similar carboxylation reaction to be catalytic in nickel.[27] In this case, the reaction was completed electrochemically, and the stoichiometric reductant was in the form of direct electron transfer. The reactions were completed using a gold or glassy-carbon electrode and a sacrificial magnesium counter electrode in DMF containing tetrabutylammonium tetrafluoroborate as a supporting electrolyte. In this work, the electrochemical behavior of $Ni(bpy)_3(BF_4)_2$ was studied both in the absence and presence of alkyne and $CO_2$ (Figure 5). The electrochemical reduction of only catalyst (Figure 5a) exhibited a two electron reduction in going from a Ni(II) species to a Ni(0) species at -1.2 V vs. SCE. At -1.9 V a single electron reduction occurred, and finally the

[27] Dérien, S.; Duñach E.; Périchon, J. *J. Am. Chem. Soc.* **1991**, *113*, 8447.

reduction of free bpy ligand occurred at -2.2 V. Upon introduction of alkyne and $CO_2$ (Figure 5d), the two electron reduction is shifted anodically to -1.15 V and becomes irreversible, indicating a reaction between the electrochemically generated Ni(0) species and the alkyne and $CO_2$.

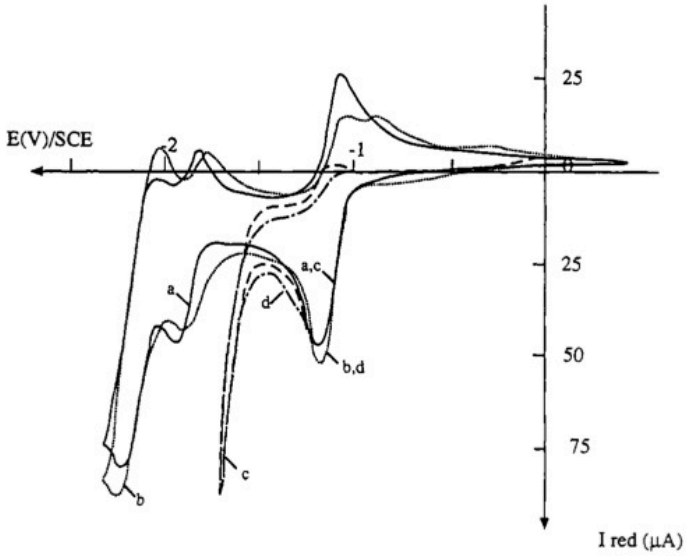


**Figure 5** Adapted from reference 25. Cyclic voltammograms are shown for catalyst in DMF containing tetrabutylammonium tetrafluoroborate as a supporting electrolyte under the following conditions: a) under argon; b) in the presence of 4-octyne; c) saturated with $CO_2$; d) in the presence of alkyne and saturated with $CO_2$.

Both terminal and internal alkynes were shown to be effective in the formation of carboxylic acids, and high regioselectivities were obtained with internal alkynes (Table 1).

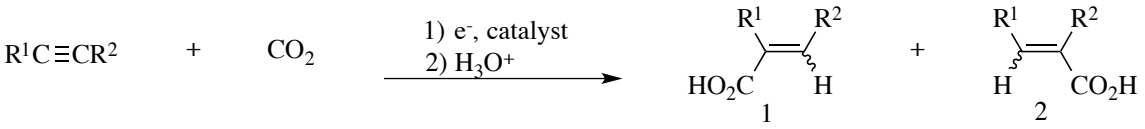


| entry | $R^1$ | $R^2$ | % carboxylation | 1:2 |
|---|---|---|---|---|
| 1 | *n*-$C_3H_7$ | *n*-$C_3H_7$ | 93 | - |
| 2 | *n*-$C_6H_{13}$ | H | 65 | 90:10 |
| 3 | *n*-$C_{12}H_{25}$ | H | 60 | 88:12 |
| 4 | c-$C_5H_9$ | H | 50 | 91:9 |
| 5 | Ph | H | 55 | 71:29 |
| 6 | Ph | $CH_3$ | 72 | 38:62 |
| 7 | Ph | Ph | 70 | - |
| 8 | Ph | $CO_2Et$ | 75 | - |
| 9 | $AcO(CH_2)_3$ | H | 65 | 50:50 |
| 10 | $AcO(CH_2)_2$ | $CH_3$ | 45 | 47:53 |
| 11 | $CH{\equiv}C(CH_2)_4$ | H | 60 | 25:50 |

**Table 1** Selectivity and isolated yields of the carboxylation of alkynes. Yields are expressed in terms of isolated methyl esters relative to the amount of reacted alkyne.

Several key aspects were studied when investigating the mechanism. A nickelacycle intermediate similar to that observed by Hoberg was isolated, and it was determined to be derived from the reactivity of the electrochemically generated Ni(0) species towards alkyne carboxylation. The influence of the sacrificial anode on this intermediate was studied, specifically, the influence of $Mg^{2+}$ ions. It was determined that the presence of $Mg^{2+}$ ions was necessary in order to open the metallacycle.

It was proposed that the opening of the metallacycle occurred by coordination of the $Mg^{2+}$ to the carboxylate group, followed by Ni-O cleavage with

protonation of the nickel-vinyl bond. The hydrogen source for this protonation was studied, and determined to come from three sources: the electrolyte, the solvent, and the residual water in the solvent. Following this information, the mechanism shown in Scheme 5 was proposed.

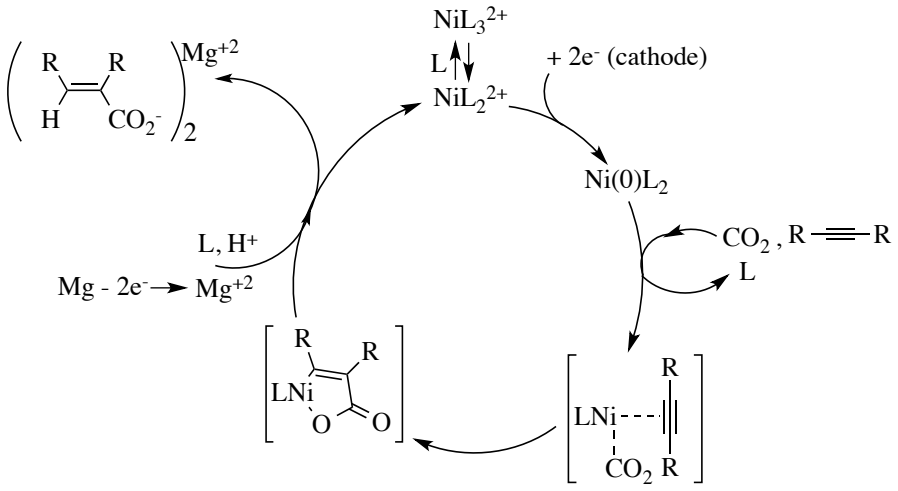


**Scheme 5** Proposed reaction mechanism of electrocarboxylation of alkynes.

In this mechanism, the Ni(II) catalyst is electrochemically reduced to the active Ni(0) state. Following this, the alkyne and $CO_2$ add to the Ni(0), forming the nickelacycle intermediate. Finally, the counterion opens the nickelacycle and a proton severs the nickel-vinyl bond, yielding the carboxylate product and regenerating the Ni(II) catalyst.

**V. SiNW shift**

These works inspired the investigation of the usage of nickel catalysts in a photoelectrochemical system. Rather than directly reducing a substrate as was done in the reduction of aryl ketones, a pre-catalyst would first be reduced in a light reaction, generating an active catalyst, which would go on to complete a dark organic reaction. In return, this new system would be able to separate the light

harvesting mechanism from the bond forming mechanism. A similar system to that used by Duñach and Périchon was used, with replacement of the electrode with a photoelectrode. By providing additional energy to the initial two-electron reduction of catalyst in the form of light, it was hoped that the amount of necessary applied potential could be reduced.

The catalytic carboxylation of 4-octyne using $CO_2$ as a primary carbon source and $Ni(bpy)_3(BF_4)_2$ (**1**) as a pre-catalyst was chosen as the reaction of interest (Scheme 6).

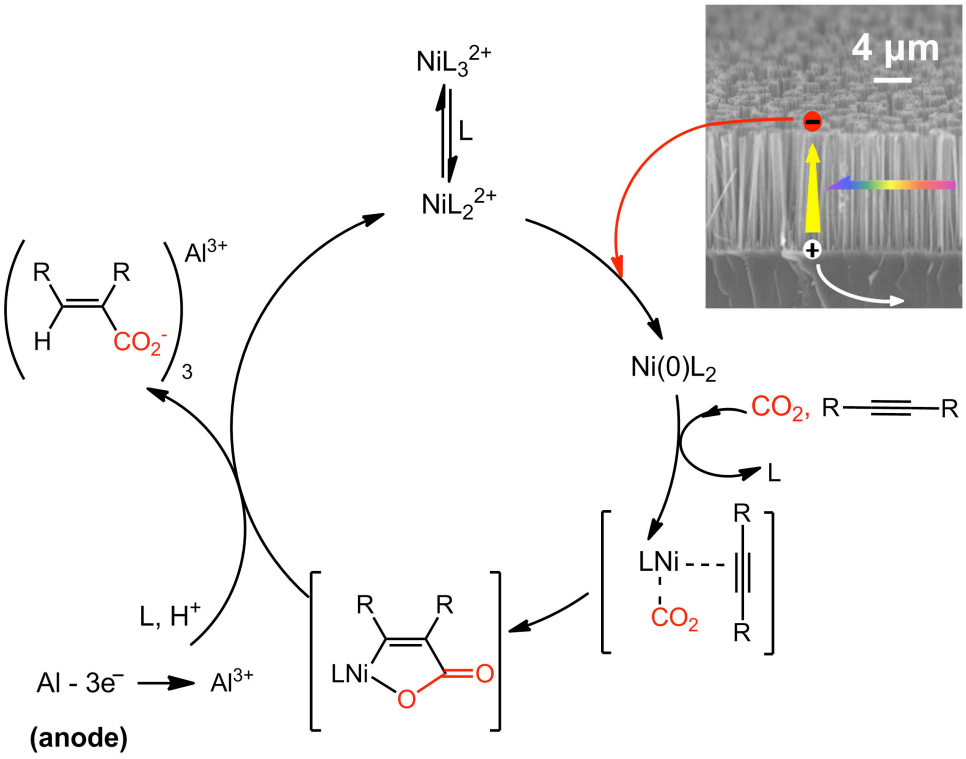


**Scheme 6** Proposed reaction mechanism of the photoelectrocarboxylation of alkynes by SiNWs.

Following the results with the aromatic ketone reduction, SiNWs were again chosen as the light-harvesting electrode. Additionally, these results were compared to those on a commonly used electrode, Pt, as well as on planar Si, a commonly used

photoelectrode. Analysis of the cyclic voltammetry of the (photo)electrodes (Figure 6a) showed an anodic shift in the redox peak potential of the Ni(II)/Ni(0) reduction on planar Si (-0.37 V) compared to Pt (-0.71 V). (All potentials are relative to the $Ag/AgI/I^-$ reference electrode, which is -0.56 V relative to the saturated calomel electrode, (SCE)).

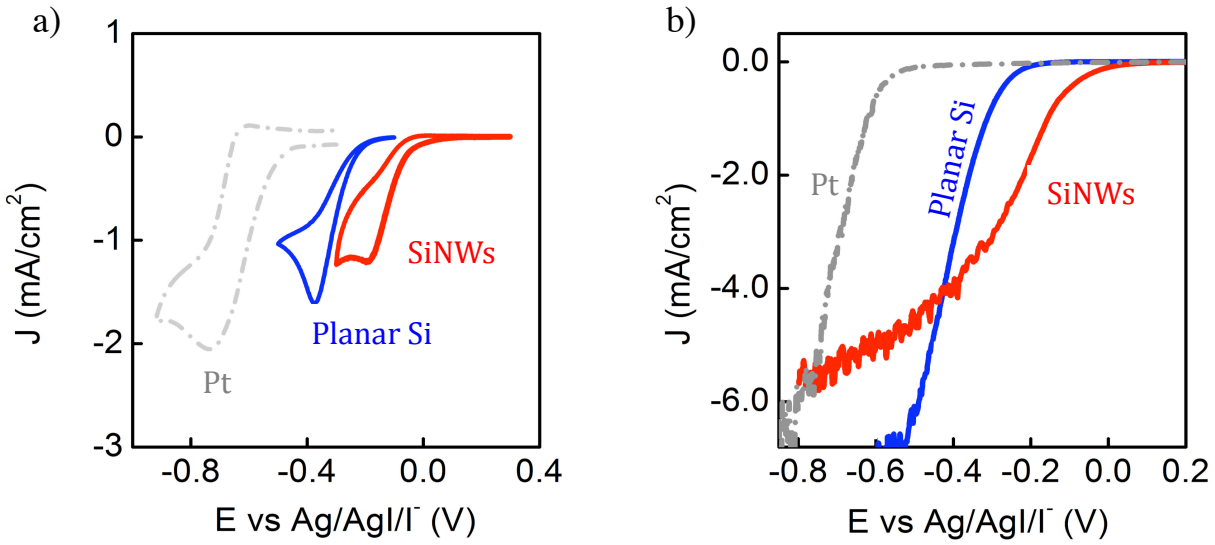


**Figure 6** Comparison of various electrodes and photoelectrodes. a) Cyclic voltammetry in acetonitrile with 0.1 M tetrabutylammonium bromide, 5 mM $Ni(bpy)_3(BF_4)_2$, and 0.05 M 4-octyne, saturated with $CO_2$. Scan rate: 5-$mVs^{-1}$. Both SiNWs and planar Si photoelectrodes were under illumination of a Xenon lamp (light intensity adjusted to 100 mW $cm^{-2}$). No measureable current was observed on the SiNWs and planar Si photoelectrodes without illumination. b) Polarization curves in the same solution but under vigorous stirring (1000 rpm).

Of note is that no anodic peaks were observed, indicating electron transfer from Ni(0) to an alkyne/$CO_2$ complex as proposed in the mechanism. This shift in reduction potential is demonstrative of the additional power gained by light due to silicon's ability to absorb light. However, we were pleasantly surprised to see a further anodic shift in going from planar Si to SiNWs (-0.19 V).

The magnitude of this shift can be further demonstrated in comparing the polarization curves on Pt, planar Si, and SiNWs (Figure 6b). We define the turn-on

potential ($V_{on}$) as the potential at which the current or photocurrent reaches 50 $\mu A/cm^2$. In doing so, a $V_{on}$ shift from -0.46 V to -0.20V is seen in going from Pt to planar Si, and a further shift to +0.04 V on SiNWs. These results indicate that the SiNWs produce larger photovoltages relative to planar Si (0.24 V more photovoltage on SiNWs compared to planar Si). These data were reproduced on more than six pairs of photoelectrodes, ruling out the possibility of a measurement artifact. While an anodic shift in reduction potential has been observed in going from planar Si to SiNWs, this shift is generally accounted for by reduced reflection and improved light harvesting in the nanowires.[28] Shifts due to such factors, however, are generally much smaller than the shift we see in our system. Therefore, it does not seem likely that such factors are the primary cause of our shift. Instead, we believe this shift is due to the ability of the photoelectrode material to transfer electrical charge to the catalyst.

This idea was investigated in reference to the band gap. Figure 7a shows a typical band diagram of a p-type semiconductor, and is representative of the SiNWs.

[28] Garnett, E.; Yang, P. *Nano Lett.* **2010**, *10*, 1082.

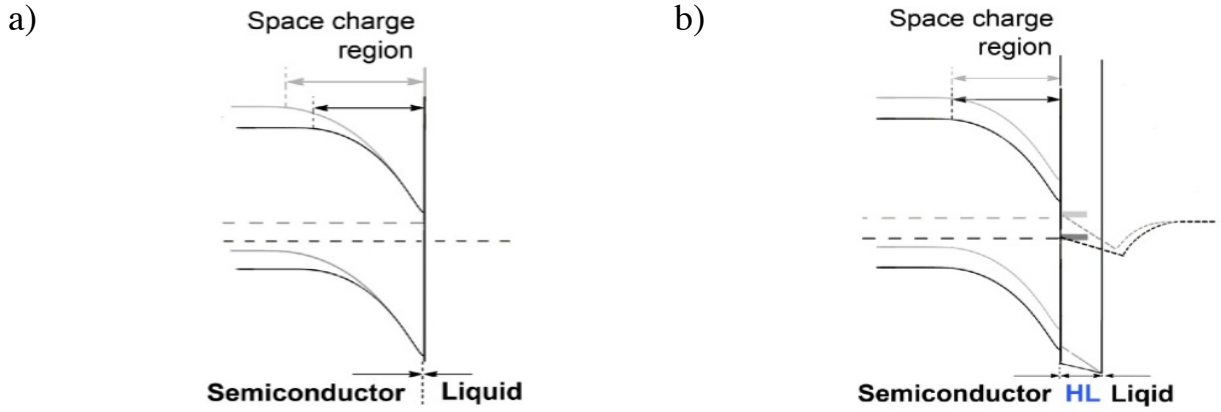


**Figure 7** Energy band diagrams of a) SiNWs and b) planar Si. A change in applied potential results in a potential drop in the space charge region on the SiNWs. On planar Si, the potential drop occurs across the Helmholtz double layer.

When the semiconductor comes into contact with an electrolyte, the potentials of each system must equilibrate, which results in the aligning of their electrochemical potentials. In order for this equilibration to occur, there must be movement of charge between the semiconductor and the solution. In our system, which uses a p-type photoelectrode, the potential of the solution starts higher than the potential of Si. As the potentials align, electrons are transferred from the solution to the semiconductor, causing an excess charge buildup near the surface of the semiconductor. The excess charge extends into the material, creating a space charge region, and has an associated electric field. This buildup of charge and resulting electric field causes this region to act as a capacitor. The band edge energies near the interface are fixed relative to the solution potential, however, away from the interface, the valence band and conduction band vary with applied potential in the same way as the Fermi level, creating band bending (in the case of p-type semiconductors, downward band banding). With increasing applied potential, the

Fermi level is raised, resulting in a smaller depletion region, and a lower capacitance. This relationship between applied potential and capacitance can be expressed mathematically by the Mott-Schottkey equation (equation 1), and graphically through a Mott-Schottkey plot.

$$C_{sc}^{-2} = \frac{2}{A^2_s q \varepsilon_0 \varepsilon N_A} \left( V_{fb} - V - \frac{kT}{q} \right)$$

**Equation 1**

Here, $C$ represents the space charge capacitance in the semiconductor, $N_A$ is the hole density, $q$ is the electron charge, $\varepsilon_0$ is the permittivity of a vacuum, $\varepsilon$ is the dielectric constant of Si, $V$ is the applied potential, $V_{fb}$ is the flat band potential, $T$ is the temperature, and $k$ is the Boltzmann constant.

The observed data for our SiNW system is shown in Figure 8a, and demonstrates a Mott-Schottkey relationship for frequencies ranging between 5 000, 10 000, and 20 000 Hz under steady-state conditions in the dark.

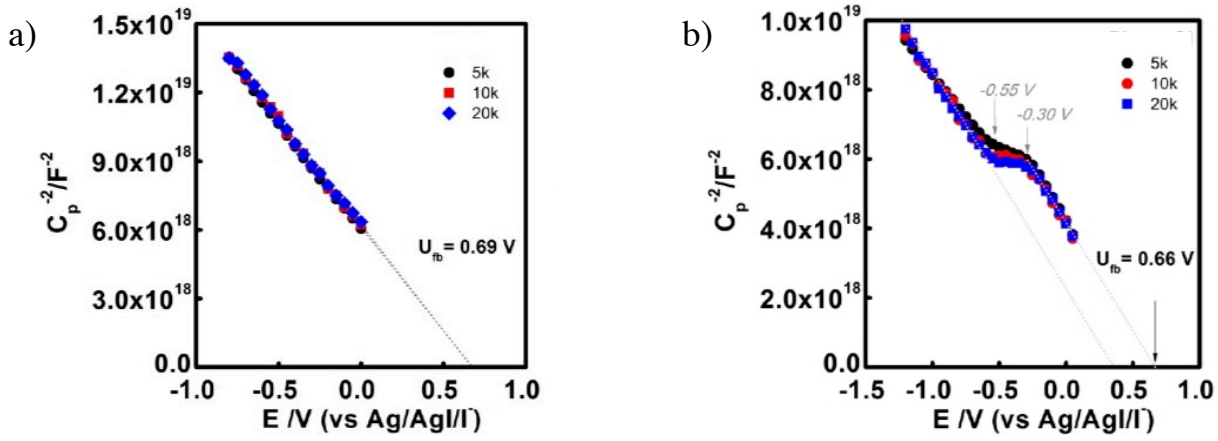


**Figure 8** Mott-Schottky plots of a) SiNWs and b) planar Si. The insets show the legends of the frequencies used. The plateau observed on planar Si (b) is attributed to the charging of the Helmholtz layer.

The linear relationship demonstrates the expected behavior of decreasing capacitance with increased applied potential, and the negative slope proves that the majority carrier is a hole, consistent with the p-type Si used. A carrier concentration of $N_A = 3.1x10^{15}$ $cm^{-3}$ was obtained, and is in excellent agreement with the information provided by the vendor of the Si substrate (resistivity: 10-20 Ω; $N_A = 10^{15}$ $cm^{-3}$). When comparing this to the Mott-Schottkey plot on planar Si (Figure 8b), however, we see an obvious deviation. In the region between -0.33 V and -0.55 V, as the applied potential is increased, the capacitance stays the same. A plateau like this is typically described in literature as a voltage region within which the applied potential drops within the Helmholtz layer instead of in the depletion region of the semiconductor (Figure 7b).[29] The most common cause of this is due to surface pinning. This, however, is not the case in our system, as one should see an increase in surface pinning with increased surface area. Instead, the plateau is only observed on pristine planar Si, and is absent on SiNWs produced by chemical etching, which are far more likely to have high surface states. We propose this phenomenon is due to some interference in the ability of the planar Si to transfer charge to the catalyst. It is well documented that the impedence to the charge transfer process is observed in polarization curves as part of the overpotential.[30] Because Ni(bpy) is not known to form covalent bonds with Si, it is likely an outer sphere mechanism, and therefore electron transfer is dependent on which surface of Si the catalyst is exposed to and

[29] Morrison, S. R. *Electrochemistry at Semiconductor and Oxidized Metal Electrodes*, Plenum, New York, **1980**.
[30] Bard, A. J.; Faulkner, L. R. *Electrochemical Methods: Fundamentals and Applications*, Wiley, New York, **1980**.

how the molecule is arranged relative to the Si surface atoms. The arrangement of the catalyst on Si is dependent on the surface potentials, and the arrangement defines the impedence charge transfer. Therefore, in order for this transfer to occur easily, the catalyst must have access to a particular Si face. The planar Si used in these reactions only allowed access to the Si(100) face, which does not favor charge transfer above -0.30 V. Rather, in this observed plateau region, the charge is being utilized to rearranging the catalyst on the surface of the semiconductor for improved charge transfer. This process is complete at -0.55 V. Of note is that between $V_{applied}$ = 0 and -0.30 V, the extracted $V_{fb}$ on planar Si, +0.66 V, is only different from that obtained on SiNWs by 0.03 V ($V_{fb}$ = +0.69 V on SiNWs). At $V_{applied}$ below -0.55 V, the potential drops by approximately 0.25 V within the Helmoltz layer, and does not contribute to the formation of the space charge region. SiNWs, on the other hand, are multifaceted in nature and thus have a variety of crystal planes present. Therefore, the catalyst has access to the favored semiconductor face, allowing for facile charge transfer.

This was further confirmed through electrochemical impedence spectroscopy measurements by fitting the data using equivalent circuits at different applied potentials. Two particularly interesting features are shown in the Nyquist plots at different applied potentials (Figure 9, see experimental section for fitting models).

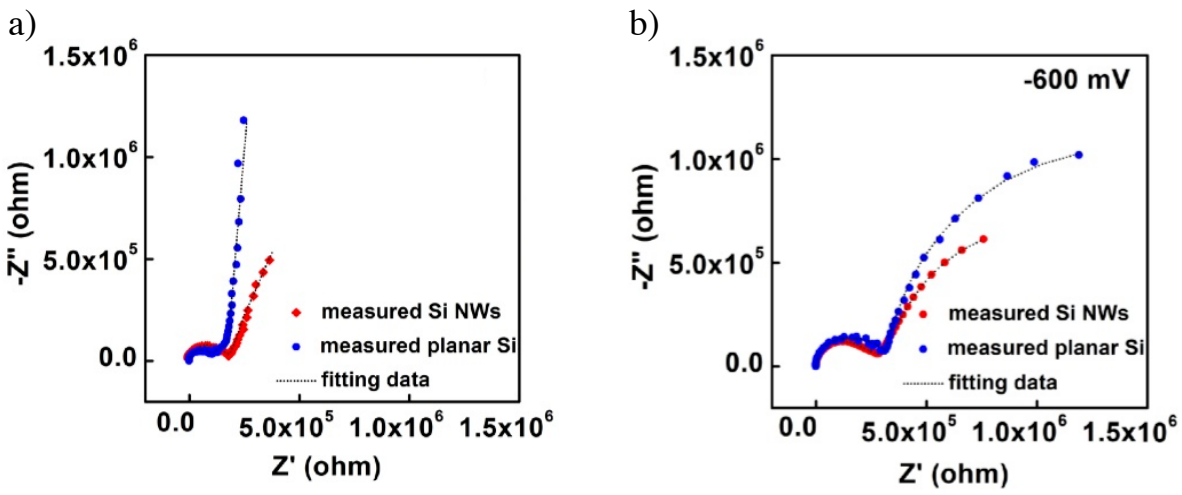


**Figure 9** Nyquist plots at 0 V (a) and -0.600 V (b) for SiNWs and planar Si. The dotted lines are fitted to the data.

The first point of interest is shown in the first semicircle region. This is the low frequency region, where capacitance in the space charge region is a dominant feature. At 0 mV, when there has been little charge transfer, the capacitance is shown to be different between the planar Si and SiNWs, as indicated in the differently sized semicircles. The capacitance decreases monotonically on the SiNWs, in contrast with the capacitance on planar Si, which remains constant between -0.30 V and -0.50 V. This is consistent with the data obtained by the Mott-Schottkey plots, and confirms that within this potential window, increased potential on planar Si drops within the solution and not in the space charge region.

The second piece of information is gained by looking at the tail of the Nyquist plots. This is the low frequency region, in which the Helmholtz layer and the solution dominate the features. It is observed that at 0 mV the resistance on planar Si ($4.03\times10^6$ Ω) is much higher than on SiNWs ($8.83\times10^4$ Ω). When increasing the applied potential to -600 mV, however, the difference in resistance on the two

systems is negligible ($1.49\times10^5\ \Omega$ and $1.60\times10^5\ \Omega$ on planar Si and SiNWs respectively, Table 2). This confirms that, at low applied potentials, it is indeed more difficult to transfer charge from the planar Si to catalyst than from SiNWs to catalyst.

a) Planar Si

| | $C_{SC}$ | $R_{SC}$ | $C_{SS}$ | $R_{SS}$ | $C_{dl}$ | $R_{dl}$ | $C_{n1}$ | $R_{n1}$ |
|---|---|---|---|---|---|---|---|---|
| **0 mV** | 7.46E-10 | 1.42E7 | 8.89E-8 | 1.15E5 | 2.82E-8 | 4.03E6 | 8.23E-7 | 9.05E4 |
| **-300 mV** | 5.60E-10 | 3.10E6 | 4.01E-8 | 2.15E5 | 4.17E-9 | 2.65E5 | 5.28E-8 | 2.43E5 |
| **-500 mV** | 5.87E-10 | 3.08E6 | 3.91E-8 | 2.12E5 | 4.50E-9 | 1.95E5 | 2.28E-8 | 3.90E5 |
| **-600 mV** | 5.31E-10 | 2.30E6 | 6.40E-8 | 2.42E5 | 2.60E-9 | 1.49E5 | 3.38E-8 | 4.00E5 |

b) SiNWs

| | $C_{SC}$ | $R_{SC}$ | $C_{SS}$ | $R_{SS}$ | $C_{dl}$ | $R_{dl}$ | $C_{n1}$ | $R_{n1}$ | $C_{n2}$ | $R_{n2}$ |
|---|---|---|---|---|---|---|---|---|---|---|
| **0 mV** | 7.29E-10 | 1.58E6 | 2.17E-7 | 1.60E5 | 2.17E-8 | 8.83E4 | 7.72E-7 | 4.47E5 | 9.01E-8 | 9.94E4 |
| **-300 mV** | 5.89E-10 | 1.76E6 | 1.64E-7 | 1.69E5 | 1.71E-8 | 8.73E4 | 4.95E7 | 2.87E5 | 9.80E-8 | 1.04E5 |
| **-500 mV** | 5.65E-10 | 2.46E6 | 1.33E-7 | 7.44E5 | 1.44E-8 | 1.35E5 | 2.14E-8 | 1.35E5 | 4.98E-8 | 1.31E5 |
| **-600 mV** | 5.39E-10 | 1.55E6 | 1.14E-7 | 2.55E5 | 1.12E-8 | 1.60E5 | 2.19E-8 | 4.72E5 | 2.19E-8 | 4.72E5 |

**Table 2** EIS simulation results for planar Si (a) and SiNWs (b) at different applied potentials.

This data demonstrates that when the Ni(II) species comes into contact with Si, a charge transfer pathway is established. At relatively positive potentials, on planar Si, a significant resistance exists, which disappears at negative enough potentials. Comparatively, on SiNWs, this pathway exists at these positive potentials, due to their multifaceted nature.

While the interesting phenomena of easier electron transfer observed on SiNWs was thoroughly investigated, one challenge encountered in this project was that yield of the desired product was low (Table 3).

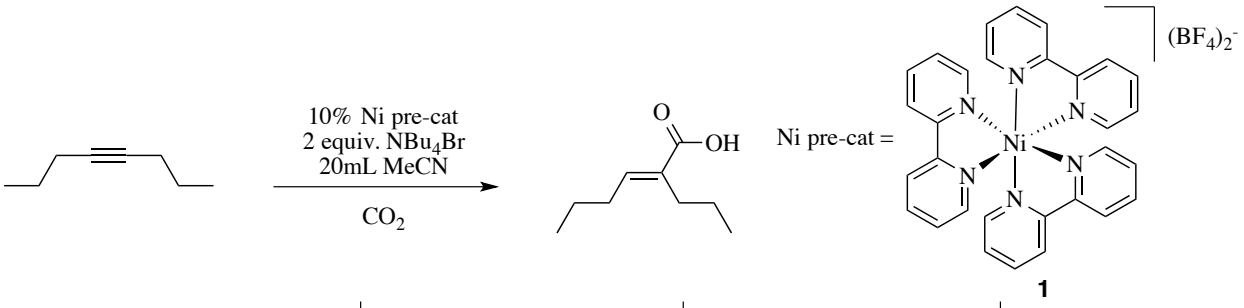


| Cathode / Conditions | Applied Potential | [a]Faradaic Efficiency | [b]Yield |
|---|---|---|---|
| SiNWs / illuminated | -0.3V | 64% | 25.9% |
| SiNWs / dark | -0.3V | No product | 0% |
| Au | -0.8V | 74% | 19.8% |

**Table 3** Faradaic efficiency and yield of the carboxylation of 4-octyne. [a]Faradaic efficiency is defined as one product mole per every 2 electron moles transferred to the pre-catalyst. [b]Yield is expressed as amount of product relative to initial starting material, and is determined by GC.

In looking at the data, it is important to distinguish between Faradaic efficiency and yield. The Faradaic efficiency is defined as one mole of product for every two electron moles transferred. Good efficiency is seen on both SiNWs, as well as a traditional electrode (in this case, Au). When looking at the yield of product, however, the amount of product generated is modest in comparison to initial amounts of starting alkyne. However, because this is a photoelectrochemical system, the low yield is actually a technical problem, not a fundamental one. This means that, theoretically, the yields should increase simply by increasing the reaction time, assuming the catalyst and electrode are stable. With increased reaction times,

however, no change in yield was observed. Because catalyst stability was a concern, the catalyst/electrode pair was investigated by exploration of a library of catalysts.

**VI. Ligand Effect**

The first approach investigated was to see if the redox potential of the system could be modified by changing the electronics of the catalyst. Introduction of electron withdrawing or electron donating groups to ligands modulate the redox potential of metal complexes.[31] Addition of an electron-withdrawing groups reduce the electron density around the metal center, making it easier to reduce. Conversely, an electron-donating group leads to a more electron-rich metal center, raising the barrier to reduction. These effects must balance with other challenges, such as catalyst stability and reversibility of electron transfer. With these modified catalysts, it was hoped that a more appropriate catalyst/semiconductor pair could be discovered, which would allow for greater product formation. Theoretically, the turnover rate of the catalyst could be increased with a more easily reduced pre-catalyst, generating more product prior to substrate degradation. The changes investigated were through modifications to the bipyridine backbone of our initial $Ni(bpy)_3(BF_4)_2$ pre-catalyst (**1**). The modified pre-catalysts are shown in Figure 9, where the ligands bathophenanthroline, 4,5-diazafluoren-9-one, 4,4'-dinitro-2,2'-bipyridine, 4,4'-di-tert-butyl-2,2'-bipyridine, and 4,4'-dimethyl-2,2'-bipyridine, respectively, were used.

[31] Sato, S.; Morikawa, T.; Kajino, T.; Ishitani, O. *Angew. Chem. Int. Ed.* **2013**, *52*, 988.

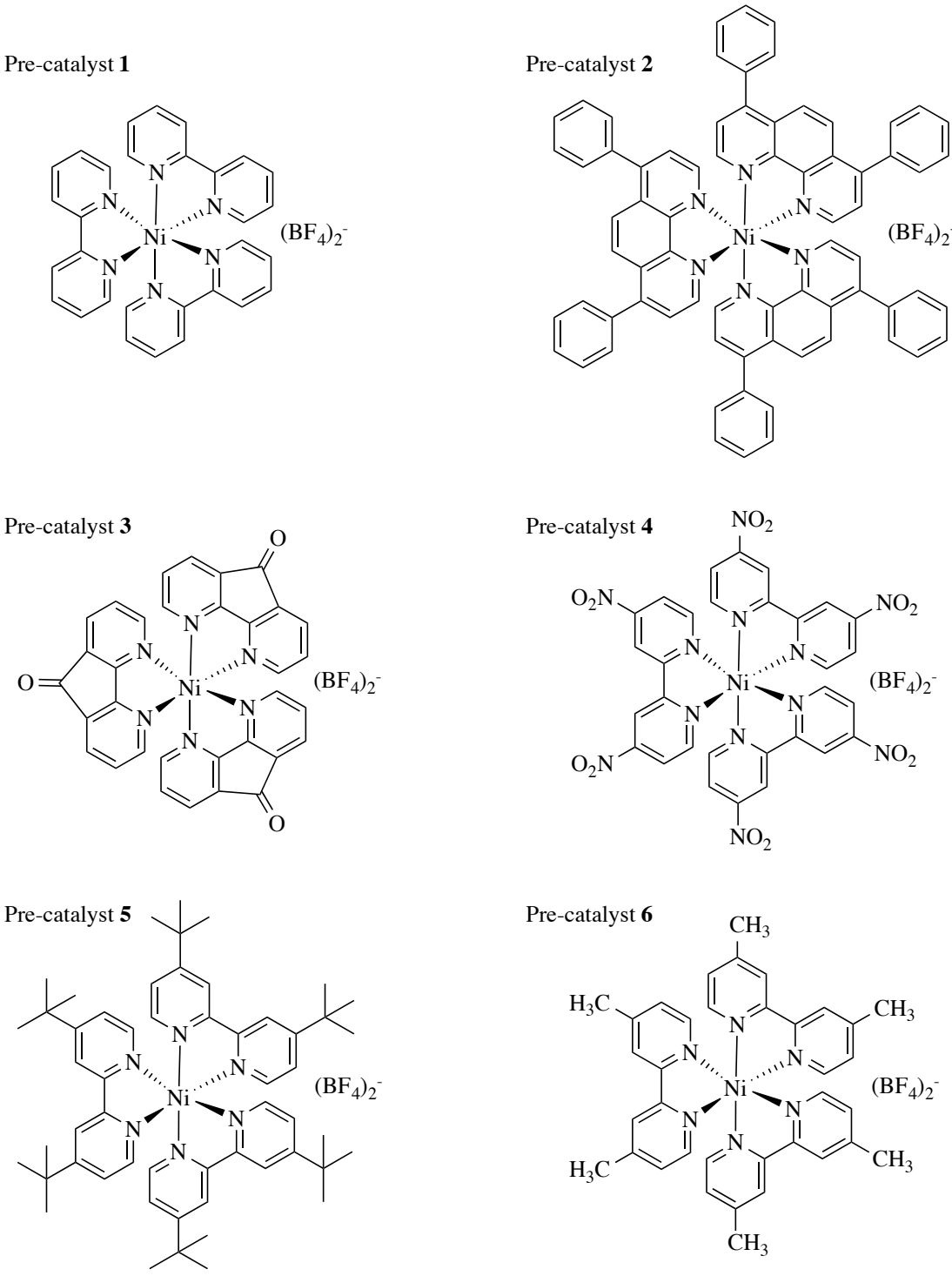


**Figure 10** Library of Ni catalysts used for $CO_2$ photofixation through alkyne carboxylation.

The primary feature investigated was the reduction peak position of the Ni(II)/Ni(0) species, as it gives direct information about how much potential is

required to reduce the Ni pre-catalyst. When looking at the application of electron withdrawing groups, a much more positive reduction peak position is shown. Conversely, there is a relative negative shift in the reduction peak position with ligands incorporating electron-donating groups. These effects demonstrate an ability to use different ligands in order to obtain a desired reduction potential in a catalytic system.

Several challenges were observed when these alternate catalysts were utilized. In most cases, the reduction peak position differences on Pt when only using catalyst and when using both catalyst and substrate were insubstantial (Figure 11).

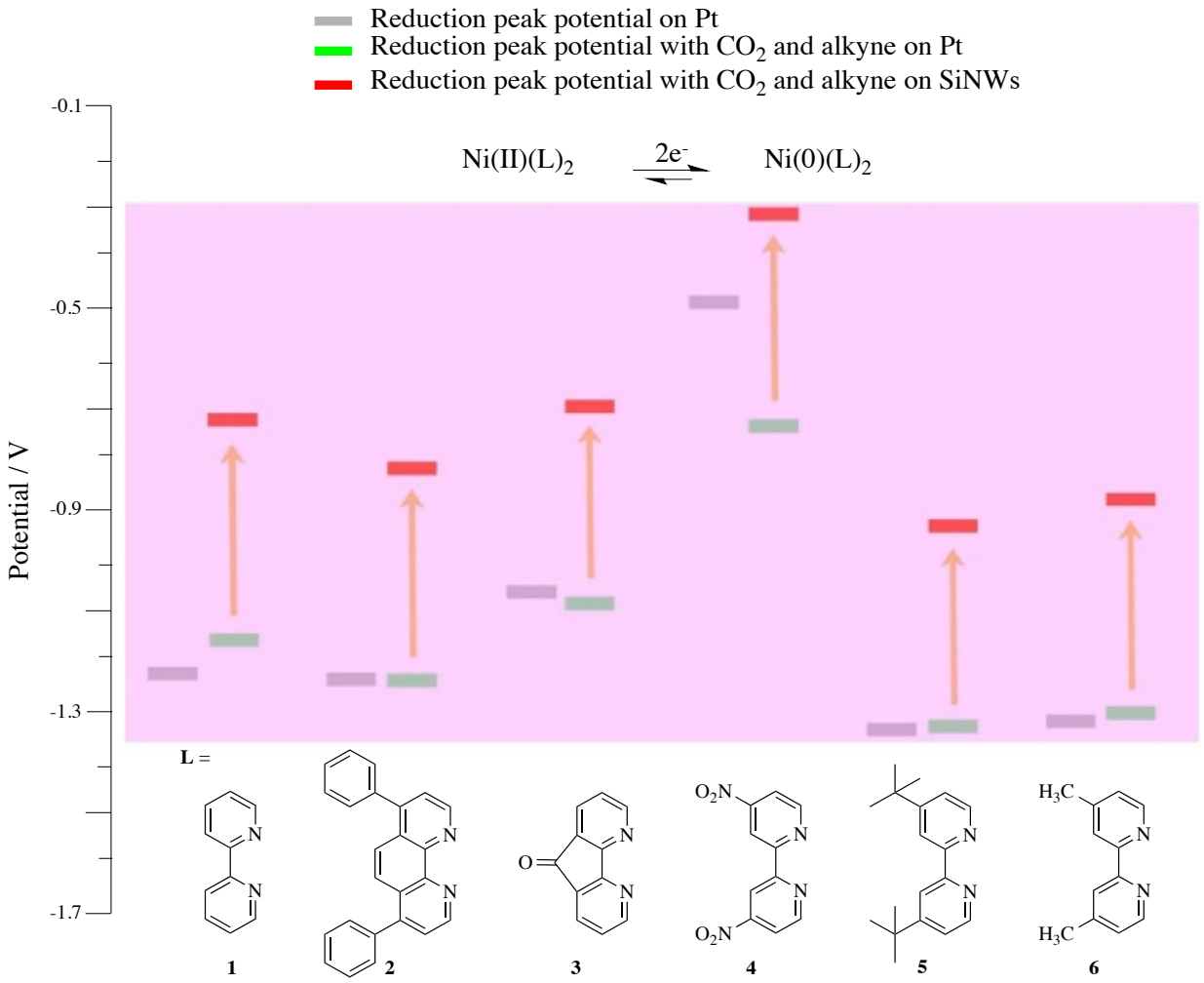


**Figure 11** Reduction peak potentials of Ni pre-catalysts. All the solutions contain 5 mM Ni pre-catalyst and 0.1 M tetrabutylammonium bromide in acetonitrile. For the conditions with substrate binding, 0.05 M 4-octyne was added with $CO_2$ gas bubbling through. SiNWs are illuminated with a 100 mW $cm^{-2}$ Xenon lamp.

The exception, however, was pre-catalyst **4**, containing strongly electron withdrawing $NO_2$ groups. The presence of substrate somehow lessened the ability of this particular catalyst to be reduced. This is represented in the more negative potential required to reduce the species in the presence of substrate. Additionally, when looking at the reduction of this pre-catalyst in the presence of substrate, a large oxidation peak is observed, indicating the pre-catalyst reduction is very reversible. This is indicative of the fact that, rather than generating product, there is

simply a rapid conversion between the Ni(II) and Ni(0) species. In addition to reversibility challenges, the challenge of yield continued to be problematic. In all cases investigated, yields using the modified pre-catalysts were mostly comparable to those of the original pre-catalyst.

**VII. Nickelacycle**

Beyond altering the catalyst's electronic structure, we also investigated the mechanism of the reaction in order to understand the origins of the low yield. Because the charge transfer from the SiNWs to the substrate is known to be facile, it was deduced that the most difficult step of the reaction was the liberation of product from the nickelacycle intermediate. To further explore this idea, it would be beneficial to begin with an isolated nickelacycle intermediate and probe the subsequent reaction. Specifically, a system using known chemistry to synthesize, isolate, and characterize a well defined intermediate could allow for careful analysis of the reaction. To complete this study, a nickelacycle previously used by the Hoberg group was chosen (**7**, Scheme 7).[32] In his work, stoichiometric amounts of nickelacycle were used to generate a variety of products.

[32] Hoberg, H.; Ballesteros, A.; Sigan, A.; Jegat, C.; Milchereit, A. *Synthesis* **1991**, *5*, 395.

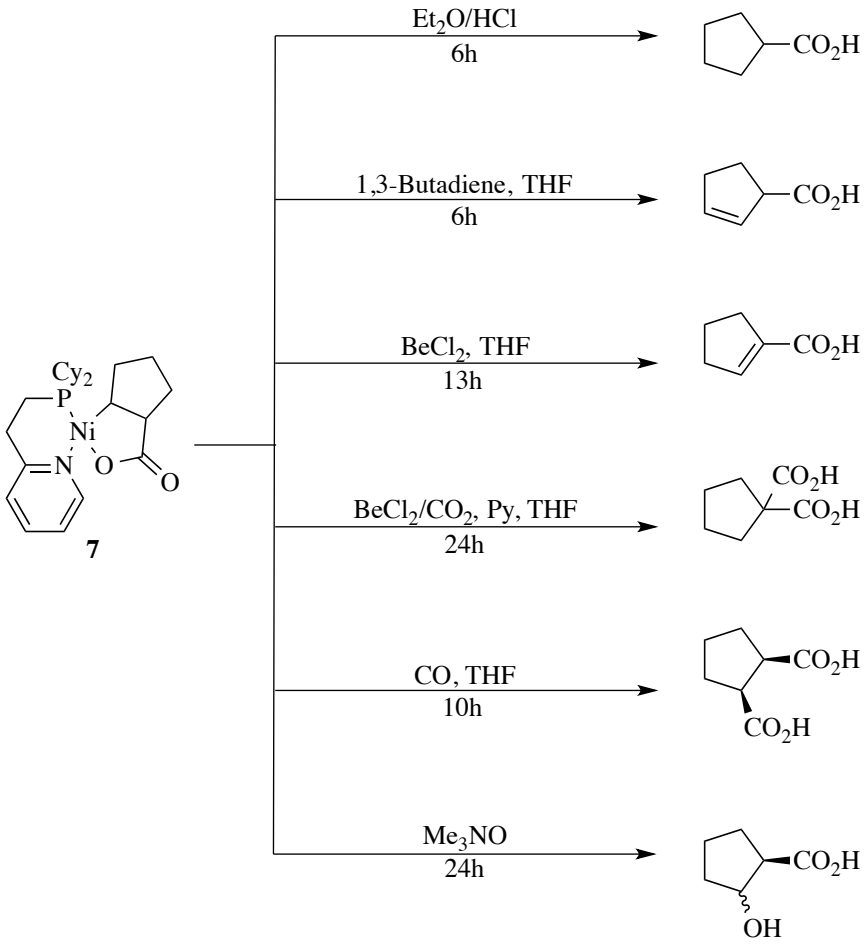


**Scheme 7** Accessible carboxylic acids from nickelacycle **7**.

In addition to allowing for the exploration the mechanism of the reaction, this particular nickelacycle presented the additional challenge of taking a stoichiometric system and turning it over, thus making it catalytic. To do so, the carboxylation of cyclopentene was chosen for investigation, which we envisioned to follow a mechanism similar to that shown in Scheme 8.

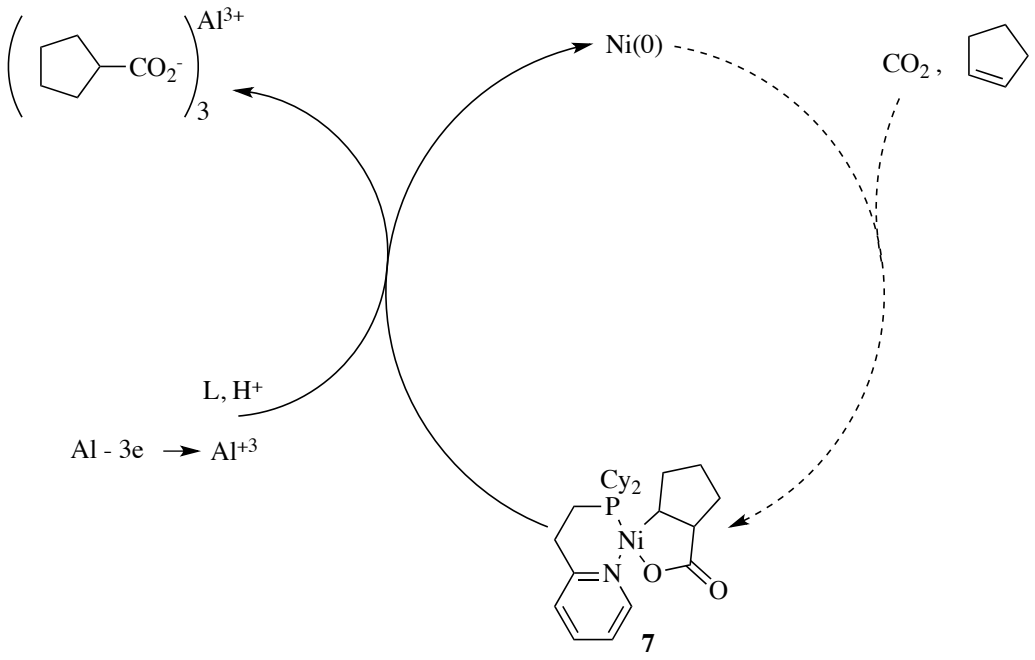


**Scheme 8** Proposed mechanism of the photoelectrocarboxylation of pentene by SiNWs.

To synthesize **7**, we first needed to make the ligand, 2-(2-(dicyclohexylphosphanyl)ethyl)pyridine. The reported synthesis of this ligand was for the diphenylphosphanyl derivative (Scheme 9).

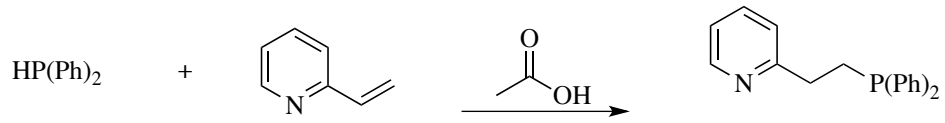


**Scheme 9**

Due to the hazards associated with dcyclohexylphosphine, however, alternative syntheses were explored. The first method was to use chlorodicyclohexylphosphine, which can be synthesized from cyclohexylmagnesium bromide and $PCl_3$. Commmercially available pyridinylethanol was converted to the alkyl bromide in the presence of $PBr_3$. Subsequent lithium halogen exchange followed by trapping

with chlorodicyclohexylphosphine should ultimately yield the desired product (Scheme 10). Unfortunately, this resulted in complete oxidation of the product.

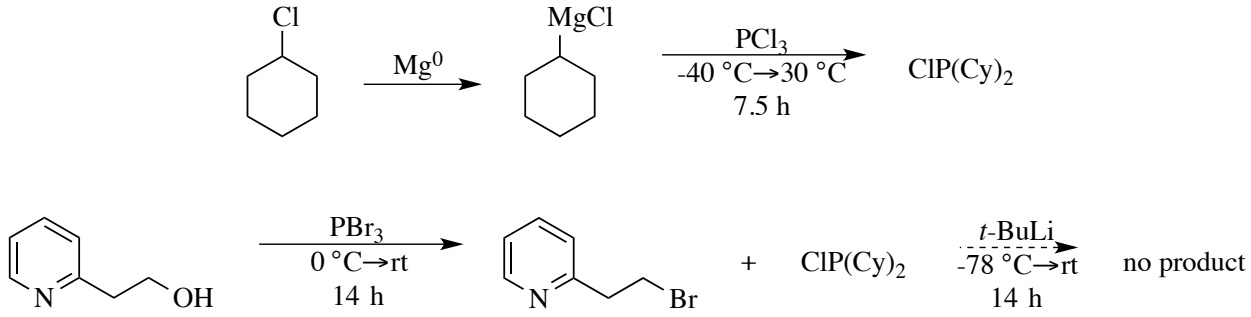


**Scheme 10**

Due to the air sensitive nature of this product, a synthesis that would allow for the protection of the phosphorous atom seemed a logical step. Based on the precedence that borane protected phosphines are more stable due to the prevention of oxidation by tying up the lone pair,[33] we initially chose to form the borane protected dicyclohexylphosphine. This was done through the protection of the chlorodicyclohexylphosphine, followed by a LAH reduction. If this could be used in the addition to vinyl pyridine, the borane-protected ligand could be generated (Scheme 11). However, after the reaction, 100% starting material was recovered, likely due to the change in electronics on the phosphorus center.

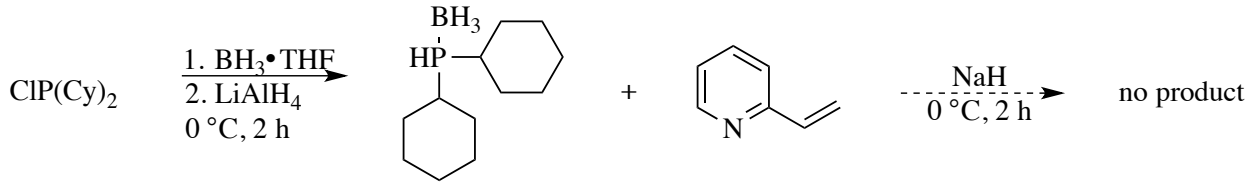


**Scheme 11**

[33] Imamoto, T.; Oshiki, T.; Onozawa, T.; Kusumoto, T.; Sato, K. *J. Am. Chem. Soc.* **1990**, *112*, 5244.

Finally, the reaction using dicyclohexylphosphine was pursued. Using Schlenk techniques, the addition of dicyclohexylphosphine to vinylpyridine was completed, and the desired ligand was provided in 59% yield by $^{31}P$ NMR (Scheme 12). In addition to the ligand, unreacted dicyclohexylphosphine, dicyclohexylphosphine oxide, and oxidized ligand were present. To allow for purification, the ligand was borane protected, resulting in an air-stable white solid in 39% yield after purification. Finally, under air-free conditions, a DABCO deprotection yielded over 90% of the deprotected ligand by $^{31}P$ NMR.

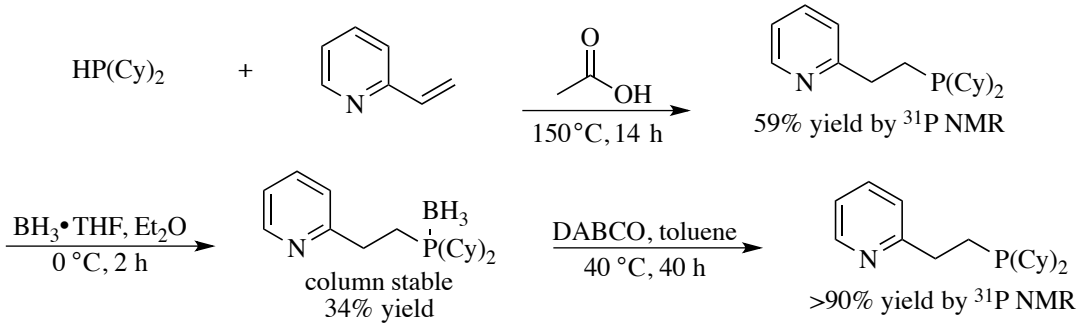


**Scheme 12**

With this material in hand, nickelacycle **7** was synthesized. Utilizing $Ni(COD)_2$ as a Ni(0) source, the complexation was completed under a $CO_2$ atmosphere at atmospheric pressure in the presence of 25 equivalents of cyclopentene (Scheme 13).

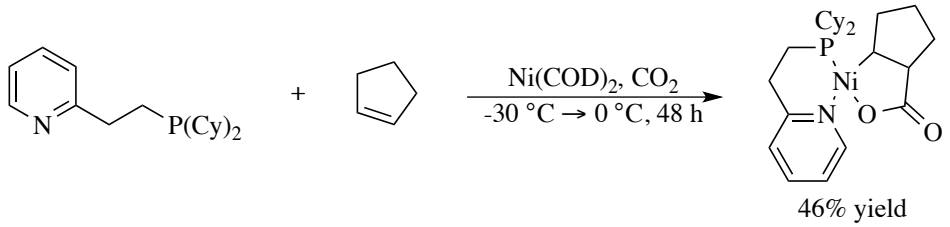


**Scheme 13**

It was hoped that, by subjecting the nickelacycle to our reaction conditions, further insight could be shed on the cleavage of product from the metal center. Unfortunately, when looking at the reduction of the nickelacycle, it was found that the reduction in going from Ni(II) to Ni(0) occurred at a very negative potential (Figure 12).

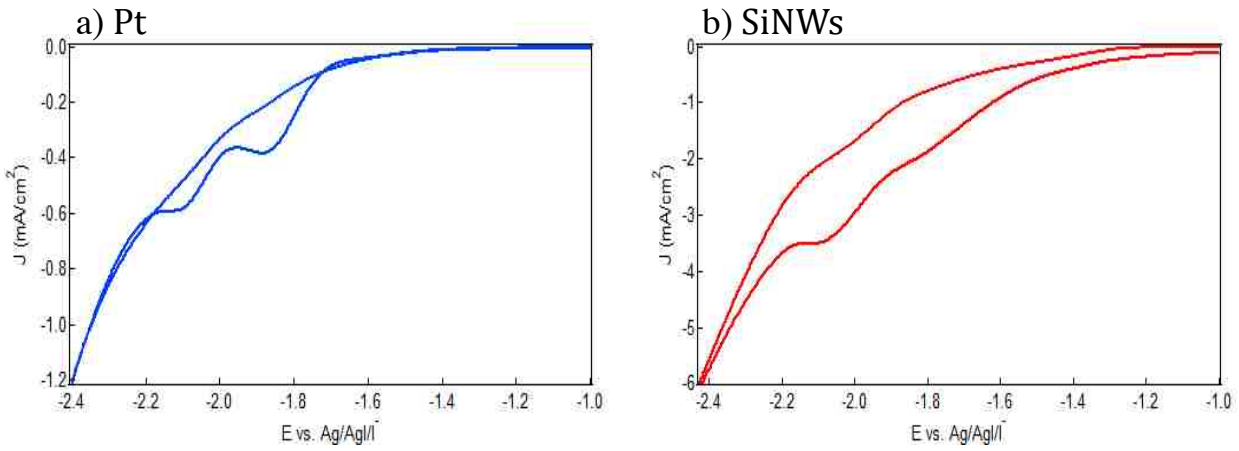


**Figure 12** Cyclic voltammetry in acetonitrile with 0.1 M tetrabutylammonium bromide and 5 mM Nickelacycle **7**, saturated with $CO_2$ on a) Pt and b) SiNWs. SiNWs were under illumination of a Xenon lamp (light intensity adjusted to 100 mW $cm^{-2}$).

Specifically, the reduction took place at a more negative potential than the direct reduction of $CO_2$, which would result in a very complicated reaction mixture. Additionally, in going from Pt to SiNWs, no major shift in the reduction potential was seen, as was observed in our previous system.

## VIII. Conclusions

The use of light as an energy source and $CO_2$ as a carbon source allows for the incorporation of readily available and prevalent materials. The incorporation of a catalyst in a photoelectrochemical system has been shown to allow for the separation of a light harvesting motif from a bond forming one, similar to

photosynthesis, allowing for the careful control of the synthesis of a useful organic molecule. In doing so, it was demonstrated that dramatically different reactivity may be observed between planar Si and SiNWs, and the multifaceted nature of SiNWs proved to be advantageous to our photoelectrochemical system. The change in necessary applied potential to reduce a catalyst was explored through ligand tuning, lending to the idea of choosing an appropriate catalyst/electrode pair for a particular system. Ultimately, it has been shown that, in a photoelectrochemical context, SiNWs may be advantageous over planar Si past greater light absorption, and can be applied to a synthetically useful system.

## IX. Experimental

### General Considerations

Unless otherwise noted, all reagents were obtained commercially and used without further purification. Flash column chromatography was performed using EMD Silica Gel 60 (230-400 mesh) and ACS grade solvents as received from Fischer Scientific. All experiments were performed in oven or flame-dried glassware under an atmosphere of nitrogen or argon using standard syringe and cannula techniques, except where otherwise noted. All reactions were run with dry, degassed solvents dispensed from a Glass Contour Solvent Purification System (SG Water, USA LLC). $^{1}H$, $^{13}C$, and $^{31}P$ NMR were performed on either a Varian Gemini 400 MHz or a Varian Gemini 500 MHz spectrometer. Deuterated solvents were purchased from Cambridge Isotope Lab and stored over 3Å molecular sieves. $C_6D_6$ was degassed by three successive freeze-pump-thaw cycles and stored over 3Å molecular sieves in a dry box under a nitrogen atmosphere. All NMR chemical shifts

are reported in ppm relative to residual solvent for $^{1}H$ and $^{13}C$ NMR. Coupling constants are reported in Hz. HRMS was generated in Boston College facilities.

Catalyst and Ligand Synthesis

**Nickel pre-catalyst general procedure.** To a flame-dried, 100 mL, round-bottom flask was added, successively, $Ni(BF_4)_2 \bullet 6H_2O$ (2.01 g, 5.88 mmol), EtOH (40.0 mL), and ligand (2.76 g, 17.7 mmol). The reaction was stirred at room temperature for one hour. The resultant precipitate was filtered, washed with $Et_2O$, and dried overnight under reduced pressure (4.00 g, 97%).

**4,5-Diazafluoren-9-one.** 1,10-phenanthroline (3.60 g, 20.0 mmol) and KOH (3.70 g, 65.3 mmol) were dissolved in $H_2O$ (270 mL) and heated to 100°C. A hot solution of $KMnO_4$ (9.18 g, 58.1 mmol) in $H_2O$ (145 mL) was added over 3 hours. The reaction was stirred for an additional 10 minutes. The solution was filtered hot, and the filtrate was cooled and extracted with chloroform (3 x 75.0 mL). The combined organic layers were dried over anhydrous $MgSO_4$, filtered, and concentrated under reduced pressure. The title compound was recrystallized with acetone and isolated as yellow crystals (1.38 g, 38%). Spectral data matched data reported in literature.[34]

**Dicyclohexyl(2-ethylpyridine)phosphine-borane.** The reaction was run using Schlenk techniques. 2-Vinylpyridine (1.07 mL, 9.89 mmol) and acetic acid (85.0 μL, 1.48 mmol) were sparged with argon, and added to dicyclohexylphosphine (2.00 mL, 9.89 mmol). The reaction was heated to 150°C under a reflux condenser overnight. The resulting yellow oil was taken up in dry MeOH and neutralized with solid $K_2CO_3$. The reaction was then filtered and concentrated under reduced

[34] Wong, K.-T.; Chen, R.-T.; Fang, F.-C.; Wu, C.-C.; Lin, Y.-T. *Org. Lett.* **2005**, *7*, 1979.

pressure. The crude product was then suspended in $Et_2O$ and cooled to 0°C. A solution of borane in THF (1.0 M, 10.9 mmol) was added and the reaction was stirred at 0°C for two hours. The reaction was then quenched with ice-cold water and extracted with $Et_2O$. The combined organic layers were washed with brine, dried over $MgSO_4$, filtered, and concentrated under reduced pressure. Column chromatography (30% $CH_2Cl_2$:Hex) afforded a white solid (0.63 g, 34%). **$^1$H NMR** ($CDCl_3$, 500 MHz) δ 8.54 (d, 1H, *J* = 4.89), 7.60 (dt, 1H, *J* = 1.96, *J* = 7.83), 7.19 (d, 1H, *J* = 7.83), 7.13 (m, 1H), 2.30 (m, 2H), 2.02 (m, 2H), 1.18 – 1.91 (m, 22H), -0.02 – 0.79 (m, 3H); **$^{13}$C NMR** ($CDCl_3$, 125 MHz) δ 161.1, 149.5, 136.7, 123.0, 121.6, 32.3, 32.0 (d, $J_{P\text{-}C}$ = 32.4), 27.1, 27.0 (d, $J_{P\text{-}C}$ = 2.90), 26.9 (d, $J_{P\text{-}C}$ = 2.86), 26.1, 18.9 (d, $J_{P\text{-}C}$ = 30.5); **$^{31}$P NMR** ($CDCl_3$, 202 MHz) δ 25.21; **HRMS** (DART-TOF) calcd. for $C_{19}H_{35}B_1N_1P_1$ $[M+H]^+$: 318.2522, found: 318.2529.

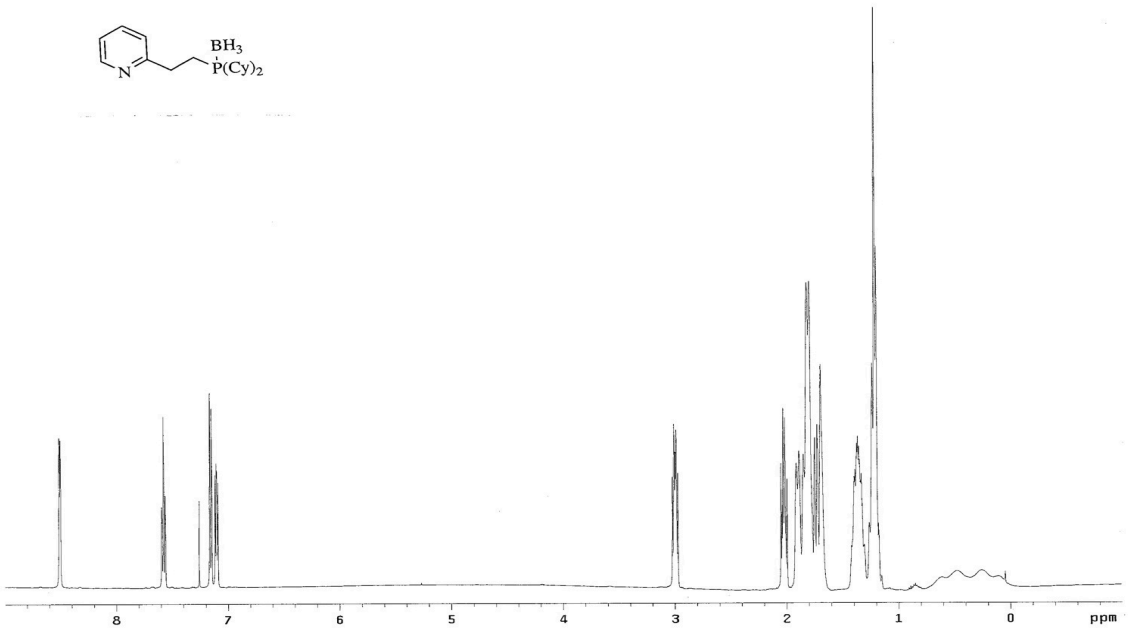
BH3
P(Cy)2
N
8
7
6
5
4
3
2
1
0
ppm

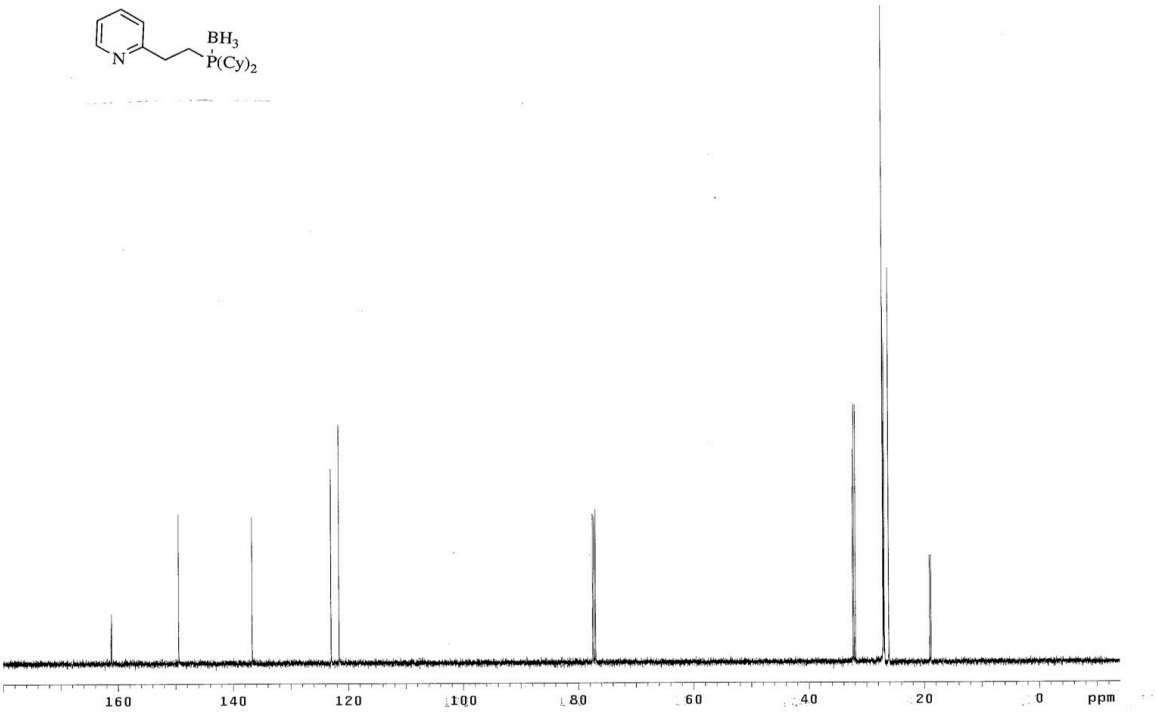
BH3
P(Cy)2
N
160
140
120
100
80
60
40
20
0
ppm

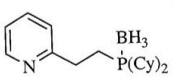


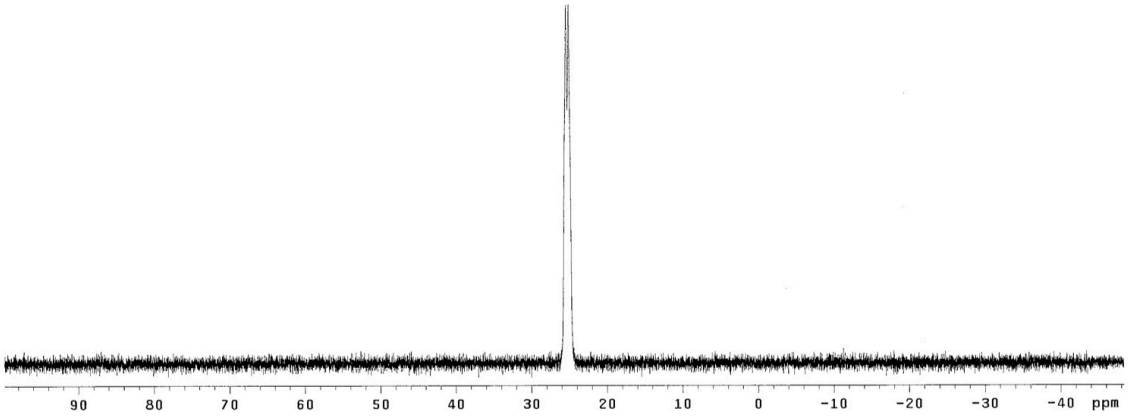


**2-(2-(dicyclohexylphosphanyl)ethyl)pyridine.** Under an inert atmosphere, dicyclohexyl(2-ethylpyridine)phosphine-borane (0.32 g, 1 mmol) was dissolved in toluene (2.00 mL) and DABCO (1.35 g, 12 mmol) was added. The reaction was heated to 40°C and allowed to stir overnight. Filtration provided the air-sensitive title compound as a clear liquid (>90% deprotection by $^{31}$P NMR. Trace amounts of oxidized ligand present.). **$^{1}$H NMR** ($C_6D_6$, 500 MHz) δ 8.53 (d, 1H, *J* = 4.41), 7.08 (dt, 1H, *J* = 1.47, *J* = 7.82), 6.83 (d, 1H, *J* = 7.34), 6.65 (m, 1H), 3.05 (m, 2H), 1.96 (m, 2H), 1.13 – 1.85 (m, 22H); **$^{13}$C NMR** ($C_6D_6$, 125 MHz) δ 163.5, 150.0, 136.2, 123.2, 121.4, 38.2 (d, $J_{P\text{-}C}$ = 21.9), 34.3 (d, $J_{P\text{-}C}$ = 15.3), 31.1 (d, $J_{P\text{-}C}$ = 15.3), 29.7 (d, $J_{P\text{-}C}$ = 8.54), 28.1 (d, $J_{P\text{-}C}$ = 11.4), 28.0, 27.3, 22.6 (d, $J_{P\text{-}C}$ = 19.1); **$^{31}$P NMR** ($C_6D_6$, 202 MHz) δ -4.4.

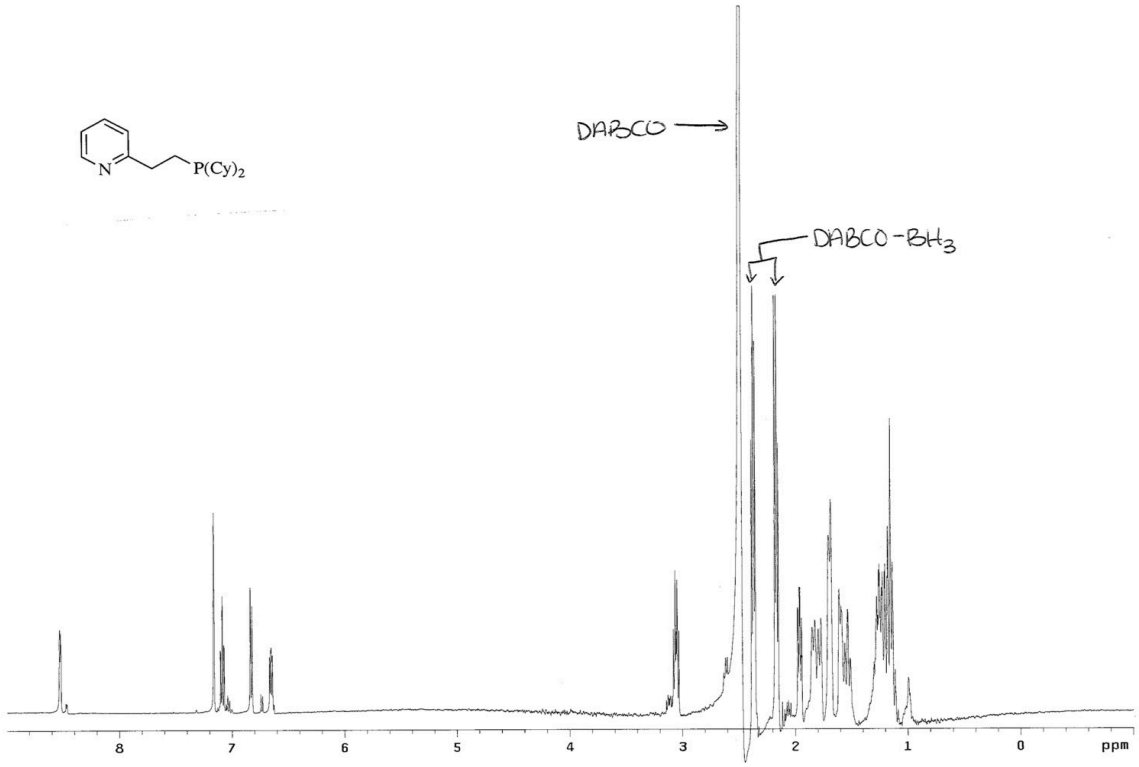
P(Cy)2
N
DABCO
DABCO-BH3
8
7
6
5
4
3
2
1
0
ppm

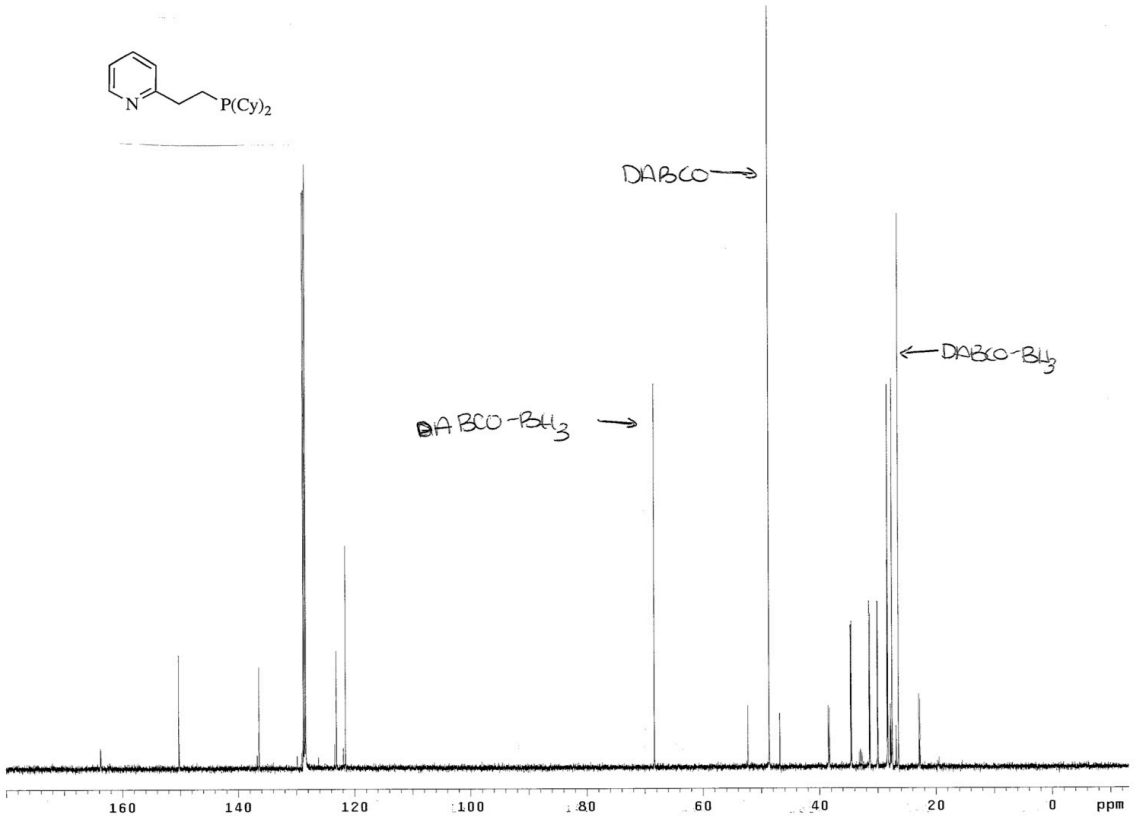
P(Cy)2
N
DABCO
DABCO-BH3
DABCO-BH3
160
140
120
100
80
60
40
20
0
ppm

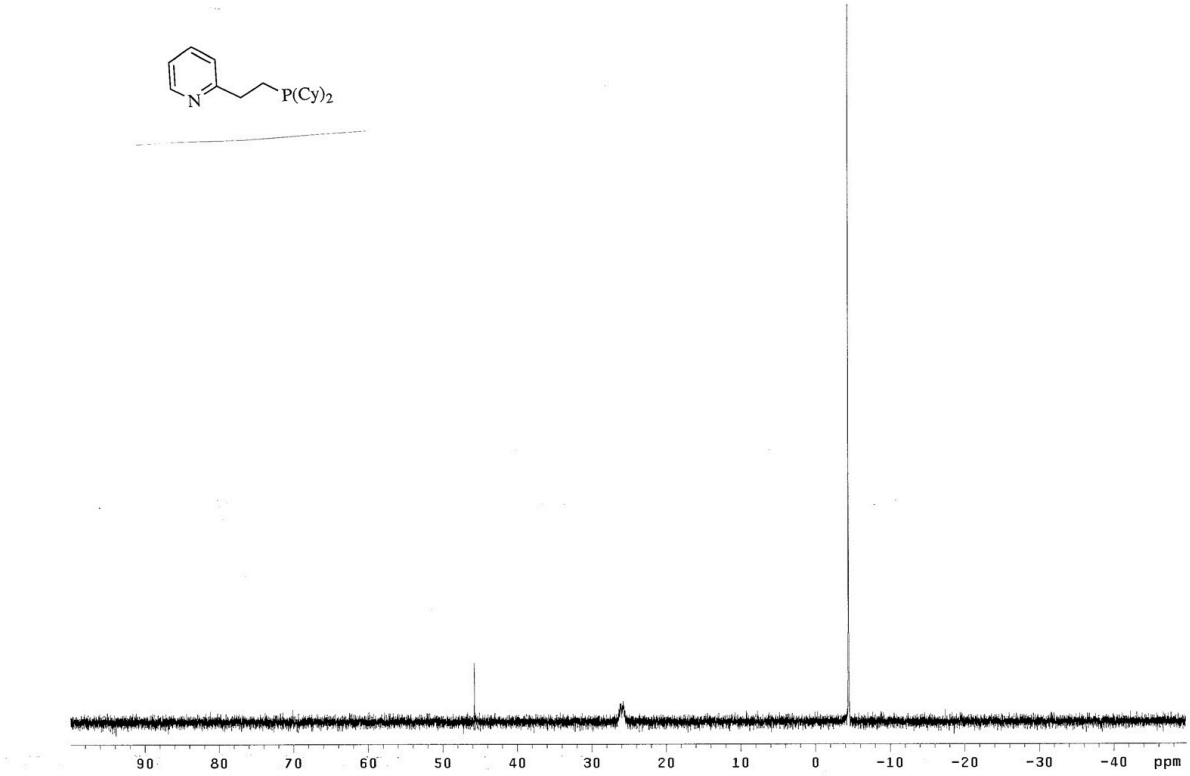


**Nickelacycle 7.** A suspension of $Ni(COD)_2$ (1.55 g, 5.63 mmol) in THF (28.0 mL) was sparged with $CO_2$, and the placed under a $CO_2$ atmosphere. The suspension was cooled to -30°C. 2-(2-(Dicyclohexylphosphanyl)ethyl)pyridine (1.71 g, 5.63 mmol) and cyclopentene (12.4 mL, 141 mmol) were added. The reaction was warmed to room temperature and allowed to stir for 48 hours. The resulting yellow precipitate was filtered under an inert atmosphere, and washed with $Et_2O$. The nickelacycle was recrystallized with $CH_2Cl_2$/pentane and isolated as a yellow powder (1.23 g, 46%). Spectral data matched data reported in literature.[35]

Photoelectrochemical (PEC) and Electrochemical Impedence Spectroscopy (EIS) Characterizations

[35] Hoberg, H.; Ballesteros, A.; Sigan, A.; Jegat, C.; Milchereit, A. *Synthesis* **1991**, *5*, 395.

**General Procedure.** PEC and EIS experiments were carried out using a CHI 609D Potentiostat. A three-electrode configuration was used, in which a Ag/AgI wire soaked in 0.1 M tetrabutylammonium iodide acetonitrile solution was used as the reference electrode, a piece of high-purity Al foil (99.9995%, Alfa Aesar, USA) served as the counter electrode, and SiNW (or planar Si) based photoelectrodes were used as the working electrode. The electrolyte solution was composed of $Ni(bpy)_3(BF_4)_2$ (0.07 g, 0.10 mmol) catalyst and tetrabutyl ammonium bromide (0.66 g, 2.05 mmol) (≥99.0%, Sigma-Aldrich, USA) in acetonitrile (20.0 mL). $CO_2$ (Airgas, USA; flow rate: 120 SCCM) was continuously bubbled through the solution. A 150 W Xenon lamp (model 71228, Newport, USA) equipped with an AM 1.5G filter and illumination intensity calibrated to be 100 mW $cm^{-2}$ by a Si photodiode (UV 005, OSI, optoelectronic, USA) was used as the light source. The scan rates for both CV and IV curves were 50 mV $s^{-1}$. EIS measurements were done with an electrolyte solution of $Ni(bpy)_3(BF_4)_2$ (0.07 g, 0.10 mmol) catalyst and tetrabutyl ammonium bromide (0.66 g, 2.05 mmol) in acetonitrile (20.0 mL) without illumination. Frequency range was from $10^5$ Hz to 1 Hz.

***(E)*-2-propylhex-2-enoic acid characterization.** The crude reaction mixture was transferred to a new 100 mL round-bottom flask and was concentrated *in vacuo* to remove acetonitrile. The reaction was quenched by the addition of 6N HCl (9 mL) and was extracted with $Et_2O$ (4 x 20 mL). The combined organic layers were dried over $Mg_2SO_4$, filtered, and concentrated under reduced pressure. **$^1$H NMR** ($CDCl_3$, 500 MHz) δ 11.5 (s, 1H), 6.9 (t, 1H), 2.3 (t, 2H), 2.2 (q, 2H), 1.4-1.5 (m, 4H), 0.9-1.0

(m, 6H); **$^{13}$C NMR** ($CDCl_3$, 500 MHz) δ 174.0, 145.9, 132.2, 31.2, 28.9, 22.9, 22.5, 14.4; **HRMS** (DART-TOF) calcd. for $C_9H_{17}O_2$ $[M+H]^+$: 157.1233, found: 157.1229.

SiNW Synthesis

SiNWs were prepared by a previously reported method. A piece of p-Si (100) wafer ($10^{15}$ $cm^{-3}$ B doped, ρ: 10~20 Ω□cm, Wafernet, USA), sequentially cleaned with acetone, methanol, and isopropanol, was further cleaned using Piranha solution of $H_2O_2/H_2SO_4$ (1:3) (Sigma-Aldrich, USA) at 90°C for 15 minutes to remove any heavy metals and organic species. Following rinsing with deionized (DI) water, the wafer was cut into approximately 1.0 cm x 4.0 cm pieces. Immersion of the pieces into an $HF/AgNO_3$ solution (4.6 M HF and 0.02 M $AgNO_3$, Sigma-Aldrich, USA) for 30 minutes at 50°C resulted in SiNWs ca. 10 μm in length. The SiNWs substrate was then cleaned by an $HNO_3$ aqueous solution (Sigma-Aldrich, USA) to remove the silver residue, and finally rinsed by DI water.

Photoelectrode Fabrication

The SiNWs substrate was immersed in HF (aqueous, 5%) for 2 minutes and dried in a stream of $N_2$. Following Al (300 nm) sputtering onto the backside of the substrate by radio frequency magnetron sputtering (AJA International, Orion 8, USA), the substrate was annealed in Ar (flow rate: 5000 standard cubic centimeters per minute, SCCM) at 450°C for five minutes in a rapid thermal processor (RTP-600S, Modular Process Tech., USA), and tinned Cu wires were fixed to the Al film by conductive epoxy (SPI supplies, USA) to form a back contact. Lastly, non-conductive hysol epoxy (Loctite, USA) was used to seal the substrate, allowing only the front surface where SiNWs reside to remain revealed.

## Reference Electrode Calibration

The homemade Ag/AgI/$I^-$ reference electrode is made by soaking a silver wire in 0.1 M tetrabutylammonium iodide acetonitrile solution in a glass tube with a porous glass tip. The potential was calibrated with SCE based on testing the same redox pair ($CoCp_2^0/CoCp_2^+$/MeCN) potential with a Pt mesh (Figure 13).

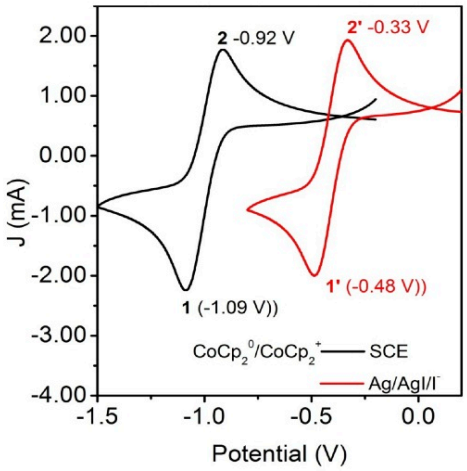


**Figure 13**

## EIS Fitting Data

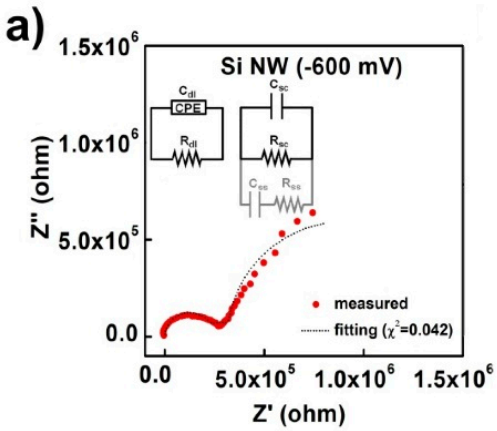

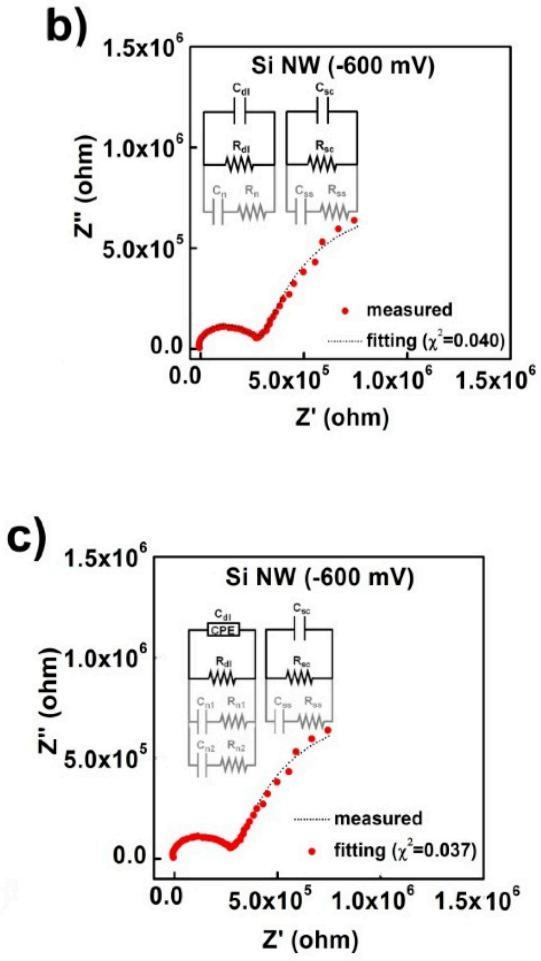


**Figure 14**

Nickel Catalyst Turnover

The fact that the nickel catalyst can turnover is one of the most important pieces of information for the reaction. Results from the following control experiments support that the catalyst indeed turns over. The first set of experiments were designed to prove that, in the absence of binding substrates such as alkynes, the Ni catalyst can't turnover, meaning that once reduced, it will remain in the Ni(0) form. The experiment was carried out by continuously applying -0.3 V potential on SiNWs with the light irradiation, but without adding binding substrates. It was

observed that the photocurrent continued dropping at a fast pace to <20% of its original value after 1.5 hours (Figure 15a). In stark contrast, when the binding substrates such as 4-octyne and $CO_2$ were available, the current degradation during the same period of time was not obvious. Moreover, CV scans afterward showed the distinct reduction peak corresponding to Ni(II) → Ni(0) conversion (Figure 15b).

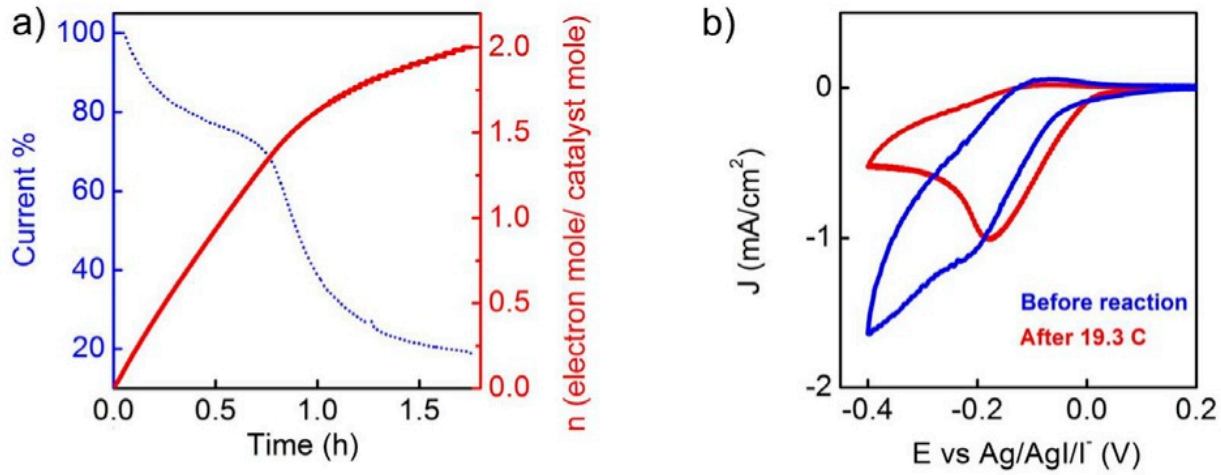


**Figure 15**

Stability of SiNW Photoelectrodes

The CV curves of SiNWs showed good reproducibility (10 continuous CV scans overlapped well in Figure 16), suggesting that the stability of both the SiNWs and the nickel catalyst were well maintained under the experimental conditions.

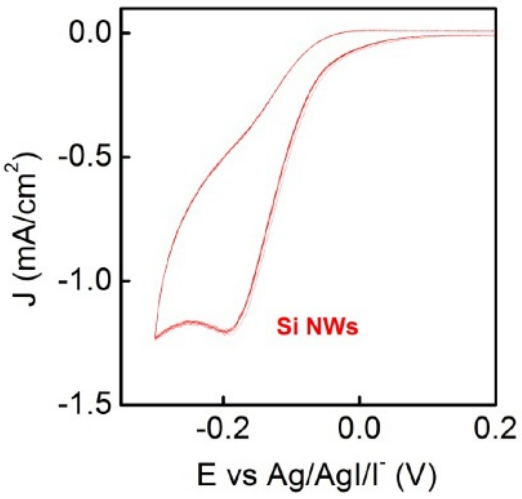


**Figure 16**